# MODELING OF PRESSURE RETARDED OSMOSIS USING THE Q-ELECTROLATTICE EQUATION OF STATE

A Thesis

by

FAHIM-BIN-ABDUR RAHMAN

Submitted to the Office of Graduate and Professional Studies of
Texas A&M University
in partial fulfillment of the requirements for the degree of

MASTER OF SCIENCE

| | |
|---|---|
| Chair of Committee, | Ahmed Abdel-Wahab |
| Co-Chair of Committee, | Marcelo Castier |
| Committee Member, | Ibrahim Galal Hassan |
| Head of Department, | M. Nazmul Karim |

July 2017

Major Subject: Chemical Engineering

# ABSTRACT

The mixing of solutions of different salinities occurs in many practical situations. A large-scale example is the mixing of river water with seawater. Such mixing processes have attracted much attention as a potential renewable energy source through a membrane-based process known as pressure-retarded osmosis (PRO). The ultimate goal of PRO units is to convert the energy released by the mixing process into mechanical or electrical power. While many researchers agree that PRO processes based on the salinity difference between freshwater and seawater are unfeasible at current conditions, more study is necessary to assess the feasibility of processes based on streams of higher salinity. One such processes is the energy recovery from desalination units by taking advantage of the mixing of discharged brine and seawater. Another process is the mixing of seawater with high-salinity produced water from oil exploration. This thesis investigates the power that can be harvested from different mixing systems such as freshwater+seawater, brine+seawater, and produced-water+seawater by PRO. To assess the performance of PRO, it is necessary to predict various thermodynamic properties such as Gibbs free energy, osmotic pressure, molar volume, entropy, and enthalpy and to calculate water fluxes across the membrane accurately. The Q-electrolattice equation of state (EOS), which extends a lattice-based fluid model for electrolyte solutions, is adopted to estimate the thermodynamic properties of the electrolyte solutions. However, the behavior of water fluxes through the membrane unit is much complicated due to concentration polarization, fouling of membrane, and reverse salt flux. Recently two very useful equations have been proposed to estimate the water and salt fluxes across the membrane that consider all of them, but the problem is the implementation of these equations into the PRO cal-

culation. Many models have been developed for PRO calculation, which calculates thermodynamic properties, water flux, and power outputs separately even though they are interdependent, thus introducing the possibility of inconsistent results. In addition, quite often, studies on this topic adopt correlations for these various properties and are based on solutions of $Na^+$ and $Cl^-$ ions only while, in practice, the solutions contain many other ions. This work develops a model to estimate the power recovery from the mixing of two solutions of different salinities by incorporating mass flux equations with Q-electrolattice EOS, which is capable of estimating all necessary thermodynamic properties and determining water and salt fluxes and power density simultaneously in a single framework. Initial investigations have been done for the solutions of $Na^+$ and $Cl^-$ ions only. Finally, the developed model is extended to solutions of multiple ions ($Na^+$, $K^+$, $Mg^{2+}$, $Ca^{2+}$, $Cl^-$ and $SO_4^{2-}$) and to multiple membrane systems.

# ACKNOWLEDGEMENTS

I would like to express my sincere gratitude to my advisors, Dr. Ahmed Abdel-Wahab and Dr. Marcelo Castier, whose expertise, understanding, generous guidance and support, and constant encouragement have helped me to a very great extent to accomplish this research work. I have been extremely fortunate to have them as advisors who gave me the freedom to explore on my own and at the same time the guidance to recover when my steps faltered. I am also highly indebted to my committee member, Dr. Ibrahim Galal Hassan, for his valuable time and constructive inputs which have improved this work.

I would like to acknowledge the contributions made by Dr. Andŕe Zuber throughout this work. I am grateful to all the staff and faculty members of the Chemical Engineering Program at TAMU-Q for enlightening me with their knowledge during the last two years. I wish to express my deepest gratitude to my friends and colleagues for making my stay at TAMU-Q a marvelous and indelible experience. I am especially thankful to my friend, Muaz Selam, for his continuous support and insightful comments to write this report. My profound appreciation goes to my parents and wife for their kind supports and words of encouragement throughout my M.S. program. In a whole, I would like to thank the Almighty Allah for keeping all circumstances in favor to me and let me complete my thesis successfully.

# CONTRIBUTORS AND FUNDING SOURCES

## Contributors

This work was supported by a thesis committee consisting of Professor Ahmed Abdel-Wahab (Chair) and Professor Marcelo Castier (Co-Chair) of the Department of Chemical Engineering and Professor Ibrahim Galal Hassan (Member) of the Department of Mechanical Engineering at Texas A&M University at Qatar.

All other work conducted for the thesis was completed by the student independently.

## Funding Sources

Graduate study was supported by a fellowship from Texas A&M University at Qatar and a dissertation research fellowship from Qatar Foundation.

# NOMENCLATURE

## List of Symbols

$A$ – Water permeability constant ($Lm^2h^{-1}bar^{-1}$)

$B$ – Salt permeability constant ($Lm^2h^{-1}$)

$c$ – Concentration ($molL^{-1}$)

$c_D$ – Concentration at draw solution ($molL^{-1}$)

$c_F$ – Concentration at feed solution ($molL^{-1}$)

$c_P$ – Salt concentration in the permeate solution ($molL^{-1}$)

$D$ – Diffusion Coefficient ($Lm^2h^{-1}bar^{-1}$)

$D_h$ – Hydraulic diameter of the flow channel

$i$ – Number of osmotically active particles

$J_s$ – Salt flux through membrane ($Lm^2h^{-1}$)

$J_w$ – Water flux through membrane ($Lm^2h^{-1}$)

$k$ – Mass transfer coefficient ($Lm^2h^{-1}$)

$K$ – Measure of resistance in the porous substrate

$l$ – Thickness of active layer

$P_D$ – Hydrostatic pressure at draw solution($bar$)

$\Delta P$ – Change of hydraulic pressure due to mass transfer through membrane ($bar$)

$R$ – Ideal gas constant ($8.314Jmol^{-1}K^{-1}$)

$R_s$ – Salt rejection

$S$ – Structural Parameter ($\mu m$)

$S_h$ – Sherwood number

$T$ – Absolute Temperature ($K$)

$\dot{V}$ – Volume flow rate ($m^3 s^{-1}$)

$\Delta\dot{V}$ – Change of Volume flow rate due to mass transfer through membrane ($m^3 s^{-1}$)

Greek Letters

$\alpha$ – Diffusion coefficient

$\upsilon$ – Degree of dissociation

$\tau$ – Tortuosity

$\epsilon$ – Porosity of membrane

$\pi$ – Osmotic pressure ($bar$)

$\pi_D$ – Bulk osmotic pressure at draw solution($bar$)

$\pi_F$ – Bulk osmotic pressure at feed solution($bar$)

$\pi_{D,m}$ – Osmotic pressure at draw side of the membrane active layer($bar$)

$\pi_{F,m}$ – Osmotic pressure at feed side of the membrane active layer($bar$)

TABLE OF CONTENTS

LIST OF FIGURES

FIGURE Page

LIST OF TABLES

TABLE Page

# 1. INTRODUCTION

## 1.1 Research statement

The global energy demand is rapidly increasing because of exponential growth in population and improved living standards. Fossil fuels (mostly crude oil, coal, and natural gas) forms the major contribution to fulfilling this demand, but their consumptions have almost reached the capacity of their maximum production [1] (see Appendix-A). This has motivated research in renewable energy. Various sustainable alternatives to fossil fuels such as the wind, solar, tidal and biomass, etc. are already being developed, but the cost associated with equipment and installation, coupled with the uneven distribution of energy throughout the year, have so far prevented them from being used widely [2, 3]. Recently, a new source of clean energy, known as 'salinity gradient energy' or 'osmotic power', has attracted much attention. The availability and predictability of osmotic power are much greater than intermittent renewables like wind and solar [4].

Water is one of the most plentiful resources on earth, but only 3% is freshwater, and 97% is salt water. According to thermodynamics, saline water is a potential source of chemical energy [5], which can be transformed into other forms of energy by mixing it with other solutions of different salinities. Initial investigations were made to harness osmotic power by mixing of seawater and river water, but the energy output from these studies was not economically feasible. At current conditions, more study is necessary to assess the feasibility of processes based on streams of higher salinity. One of such processes is the energy recovery from desalination units by taking advantage of the mixing of discharged brine and seawater. Another process is the mixing of seawater with high-salinity produced water from oil exploration.

Pressure retarded osmosis (PRO) is a membrane-based technology used for recovering energy from saline water as mechanical or electrical power. Many PRO models have been developed to estimate energy recovery from saline solutions at different salinity, pressure, and temperature conditions, but limitations exist. To access them, an efficient thermodynamic model becomes necessary to predict several thermodynamic properties in order to accurately determine the maximum possible power recovery from the PRO processes.

## 1.2 Osmotic power

'Osmotic power' is the energy derived using salinity gradients (concentration difference between two solutions of different salinities) where two sources of water with different salinities are in contact. In broad terms, it is the energy obtained by the controlled mixing of two solutions of different salt concentration (e.g. river water and seawater). Investigations have shown that approximately $2.5 - 2.7MJ$ of energy can be harnessed when $1m^3$ of freshwater flows into the sea [6, 7]. However, the challenge in exploring this energy is the development of economically feasible technology. Various technologies, such as reverse electrodialysis (RED) [**?**, 8], pressure retarded osmosis (PRO) [9, 10], capacitive mixing (CAPMIX) [11, 12], and hydrogel mixing [12], have been developed to harvest osmotic power but only RED and PRO have been implemented on the pilot scale.

Both RED and PRO are membrane-based technologies and are driven by chemical potential differences, but their operation and mechanical structure are different from each other. RED uses a stack of alternating ion-exchange membranes that allow only salt ions to permeate across the membrane and the net flux of ions is transformed into the electric current [13,14]. On the other hand, PRO utilizes a single semipermeable membrane which allows water (rather than ions) to pass through

the membrane. The expanding volume of saline solution turns a hydro-turbine that generates useful mechanical or electrical work [6, 9, 10]. Both technologies have comparable efficiencies on the recovery of osmotic power, but the cost of membranes is greater for RED than for PRO. Recently, Post et al. [15] have reported that the price of RED-membranes has to be reduced by a factor of a hundred to make the technology affordable. Furthermore, Yip et al. [**?**] have scrutinized PRO, showing that it can recover more power and achieve higher efficiencies than RED and other existing technologies. Therefore, PRO is the most promising technology to recover energy from the mixing of two solutions of different salinities.

## 1.3 Recent developments in PRO

Although Pattle [13] first reported the concept of PRO in 1954, the published materials and experimental data on PRO showed that the research to harness energy from saline water by PRO process is mostly raised in the 1970-1990 and the 2000s. Over the years, tremendous improvements happened to PRO technology, particularly after installing the first prototype power plant by Statkraft, a Norwegian power company in 2009. The plant was designed and built based on Loeb's proposal, which was operated on the mixing of freshwater and seawater, between 2009 and 2012, when it was discontinued for insufficient power production[1]. Statkraft reported that reverse salt fluxes across the membrane and fouling of the membrane along with concentration polarization were the main reasons for that unfeasible power production. Recently, researchers are working to overcome some of the complications of the PRO technology, such as concentration polarization, reverse salt fluxes through the membrane, fouling and scaling, durability, and the cost of membrane. For instance, Yip et al. [16] introduced reverse salt fluxes and fouling of the membrane in their

[1]Statkraft press center, Crown Princess of Norway to open the world's first osmotic power plant, 2009; http://www.statkraft.com

model to determine the power output of a PRO process accurately.

Most studies on PRO focus on the mixing of seawater and freshwater, but the power output based on the salinity difference between these two solutions is currently unfeasible. Researchers agree that more study is necessary to assess the feasibility of processes based on streams of higher salinity [17]. One such process is the energy recovery from desalination units by taking advantage of the mixing of discharged brine and seawater. Another process is the mixing of seawater with high-salinity 'produced water' from oil exploration [18]. However, the performance of such PRO processes depends on the accurate estimation of several thermodynamic properties such as osmotic pressure, entropy, enthalpy, liquid density, and Gibbs free energy of mixing. The Gibbs free energy of mixing provides the upper limit on the shaft work that is possible to recover from the mixing process, and osmotic pressure is necessary to establish the operating pressure at different parts of a PRO plant. Entropies and enthalpies are needed to evaluate the mechanical power of the rotary equipment involved.

Many models have been developed to accurately evaluate all of these properties, but limitations exist such as (a) most of the existing models are suitable only for low salinity solutions [12, 19–21]; (b) existing models are based on solutions of $Na^+$ and $Cl^-$ ions only whereas, in practice, saline waters contain other ions in addition to these two [21–23]; (c) finally, such models calculate thermodynamic properties and power densities (power produced per unit membrane area) separately even though they are interdependent (e.g. 'OLI software' is used to obtain solution properties, and other software/programs are used to determine mass fluxes and power density) [6, 24], thus introducing the possibility of inconsistent values for such quantities. Therefore, an effective model becomes necessary to estimate all of these properties and to determine the power density in the same framework in order to accurately

determine the maximum possible power recovery from the PRO processes.

To develop such model, a thermodynamic analysis is made in this work by incorporating the Q-electrolattice equation of state (Q-electrolattice EOS) along with recently developed equations [16] which include concentration polarization, fouling of the membrane, and reverse salt fluxes for the calculation of water and salt fluxes across the membrane. The Q-electrolattice EOS correctly evaluates all thermodynamic properties of saline solutions, and fluxes equations help to do accurate mass and energy balance in order to determine the maximum possible power recovery from a practical PRO process.

## 1.4 Motivations

Qatar is the largest producer and exporter of liquefied natural gas in the world, and it is among the top twenty oil producing countries in the world. Conversely, it has scarce natural drinking water, thus increasing the dependence on desalinated seawater to satisfy 99% of its municipal water demand[2]. As discussed before, both petroleum industries and desalination plants produce an enormous amount of contaminated saline wastewater. Direct release of these water streams to the sea has huge adverse effects on the environment. Prior to the disposal, this water has to be treated that consumes an enormous amount of energy. On the other hand, saline water is an excellent source of chemical potential, which can be converted to another form of energy. However, in practice, this water is released to the sea just after the treatment process, without any energy recovery. Therefore, the motivation of this thesis is to investigate power recovery from saline water by PRO that can be used to reduce the energy consumption in wastewater pretreatment units.

[2]Water desalination and treatment, Qatar Environment and Energy Research Institute;(accessed on 22 March 2017)

## 1.5 Research aim and objectives

The aim of this research work is to develop a model for PRO processes using the Q-electrolattice EOS to accurately predict various thermodynamic properties of saline solutions having many ions and apply this model to a wide range of concentrations, temperatures, and pressures. The ultimate goal of this study is to maximize the power recovery from a PRO system at given temperature and pressure. The various objectives associated with this aim are:

1. Implement the Q-electrolattice EOS for the calculation of osmotic pressures of NaCl solutions at various temperature, pressure and concentration conditions-verifying the results with existing models and experimental values.

2. Develop a model by combining Yip's model [16] equations for estimating water and salt fluxes with the Q-electrolattice EOS, which simultaneously renders thermodynamic properties, water and salt fluxes, and net power of the process.

3. Implement the model for a single membrane unit PRO process, with NaCl+water in both concentrated and dilute solutions-verifying the results with experimental values.

4. Extend this model for solutions of multiple ions and implement it for multiple stage membrane systems.

## 1.6 Presentation of the thesis

Based on research objectives, this thesis is distributed into six chapters as follows:

1. The first chapter (current chapter) introduces osmotic power and different technologies to harvest osmotic power, the importance of PRO modeling, the motivation for this research, and the aim and objectives of this thesis.

2. The second chapter mainly focuses on salinity gradient energy and the technologies used to harness this energy from the mixing of saline solutions. It also briefly describes the development of PRO process over the years.

3. The third chapter deals with the basic concepts of PRO technology and the development of PRO models for estimating water and salt fluxes across the membrane.

4. The fourth chapter demonstrates the basic idea of the Q-electrolattice equation of state that was used to evaluate the necessary thermodynamic properties in PRO modeling.

5. The fifth chapter discusses the formulation of the PRO model and the methodology to calculate fluxes and power density. It also illustrates the extension of the developed model from a single-stage to a multiple-stage membrane system.

6. The sixth chapter discusses the results of this thesis. At first, the modeled results are validated by comparing with the results obtained by experiments and literature models and then, studies the effects of various operating conditions on power density.

7. The final chapter summarize the conclusions drawn from this research.

# 2. SALINITY GRADIENT ENERGY

## 2.1 Osmotic process

'Osmosis' is the spontaneous transport of solvent molecules across a semipermeable membrane from the solution where the solvent has higher chemical potential (lower concentration of solute) to the solution where it has lower chemical potential (higher concentration of solute), thus equalizing the chemical potential of the solvent on both sides of the membrane. The movement of water through the membrane is driven by the chemical potential difference between the two solutions [25]. The osmotic pressure is the minimum pressure to be applied to a solution to prevent water transport across the membrane. Water transport from freshwater to seawater through a semipermeable membrane is a common example of the osmotic process, which is shown in Figure 2.1[1].

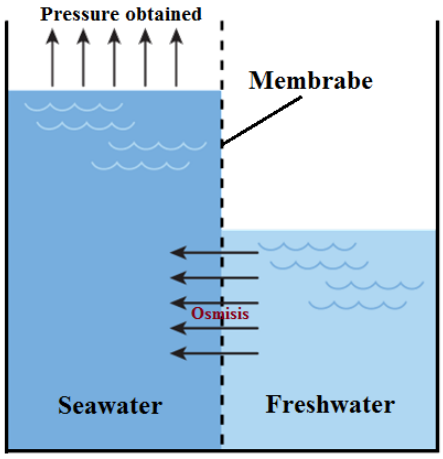


Figure 2.1: The principle of osmotic process

[1]https://en.wikipedia.org/wiki/Pressure-retarded_osmosis (accessed on 21 May 2017)

Three types of osmotic process occur when two solutions of different salinities are contacted via a semipermeable membrane: forward osmosis (FO), reverse osmosis (RO), and pressure retarded osmosis (PRO) [26]. Figure 2.2 represents the classification of osmotic processes depending on the differential osmotic pressure ($\Delta\pi = \pi_D - \pi_F$) and differential hydraulic pressure ($\Delta P = P_D - P_F$) across the membrane. The subscript $D$ and $F$ represent the draw and feed solution respectively.

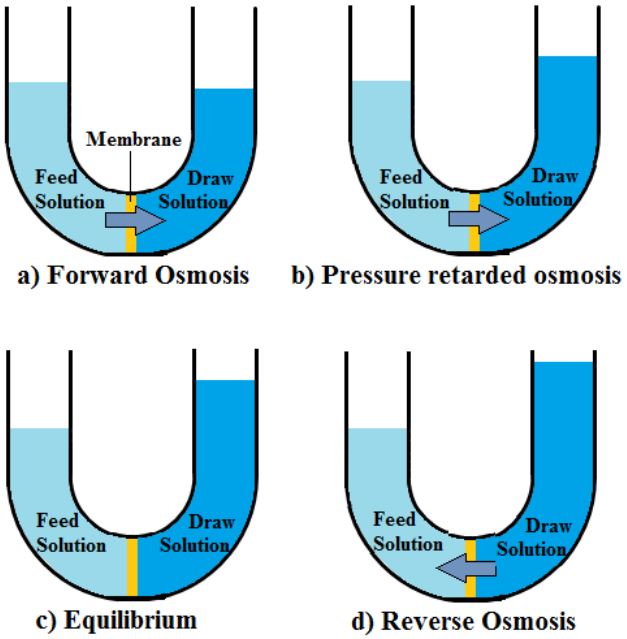


Figure 2.2: The classification of osmotic processes: a) FO ($\Delta P = 0 < \Delta\pi$); b) PRO ($0 < \Delta P < \Delta\pi$); c) Equilibrium ($\Delta P = \Delta\pi$); d) RO ($\Delta P > \Delta\pi > 0$) [17, 26]

FO is an osmotic process, while water passes through the membrane from low salinity 'feed solution' to high salinity 'draw solution' across the membrane without

any pressure difference between the solution, thus $\Delta\pi > \Delta P = 0$. In FO, the osmotic pressure difference is the main driving force to transport this water. In Fig.2.2, the height of the solution indicates the pressure inside the solution, while the dark and light color of the solutions refer to the draw and feed solution, respectively. Since $\Delta P = 0$ for FO, the height of the draw solution should be a little bit lower than the feed solution because of its higher density. If a pressure is applied to the draw solution, the water transfer through the membrane decreases and when the new pressure difference becomes greater than the osmotic pressure difference, the water starts to move from draw solution to feed solution, which is known as RO. The general condition of RO process is $\Delta P > \Delta\pi > 0$. The height of the draw solution is much higher than the height of the feed solution.

PRO is the intermediate process between FO and RO, where $\Delta\pi > \Delta P > 0$. In PRO, the pressure is applied to the draw solution (as in RO), but the water transport across the membrane is towards the draw solution (similar to FO). Therefore, $\Delta P$ gradually increases and, eventually $\Delta\pi$ decreases, which causes to reduce the water flux through the membrane. When $\Delta P$ equivalent to $\Delta\pi$, the osmotic flow will stop. This condition determines the state of equilibrium. Mathematically, at equilibrium $\Delta P = \Delta\pi$.

## 2.2 Osmotic power generation

Osmotic power is the energy per unit of time harvested from the mixing of solutions of different salinities. The most typical example of osmotic power extraction is the mixing of freshwater and seawater. When river water flows into the sea, spontaneous mixing occurs, but no energy can be harvested because the natural mixing of river water and seawater is irreversible. However, it is possible to extract this energy from the mixing if the process can be done reversibly [27]. In addition, extracted

energy increases when salinity gradient increases between the solutions. Helfer et al. [17] provided an estimate of the maximum possible power extraction by mixing of freshwater with the saline water from different sources (Table 2.1). Several techniques have been developed for the conversion of salinity gradient energy to usable mechanical or electrical power, but only PRO and RED have been implemented on pilot scale [27]. Recently, CAPMIX technology also attracted much attention for harvesting energy from salinity gradients [11, 28].

Table 2.1: Theoretical extractable energy from the mixing of freshwater with saline water from different sources [17]

| Saline water sources | Osmotic pressure | Theoretical energy | |
|---|---|---|---|
| | *bar* | $kWh.m^{-3}$ | $MJ.m^{-3}$ |
| Seawater | 27 | 0.75 | 2.7 |
| SWRO brine | 54 | 1.5 | 5.4 |
| Salt-dome solution | 316 | 8.8 | 31.6 |
| Great Salt Lake | 375 | 10.4 | 37.5 |
| Dead Sea | 507 | 14.1 | 50.7 |

### *2.2.1 Pressure retarded osmosis (PRO)*

PRO is an osmotically driven membrane technology, which harnesses the energy of mixing between two solutions of different salt concentration to produce mechanical or electrical power [14]. The principle of power extraction by PRO is demonstrated in Fig. 2.3. Two solutions of different salinities (e.g. seawater and freshwater) are brought into contact with a selectively permeable membrane, which only allows the solvent (i.e., water) to permeate across the membrane. The solvent molecules are transported through the membrane from 'feed solution' at atmospheric pressure to partially pressurized 'draw solution' due to the chemical potential difference between

them. The pressure applied to the draw solution is less than the osmotic pressure difference between draw and feed solutions. Additionally, the permeate solution increases the volume in draw solution compartment and dilutes the draw solution. The pressurized and diluted draw solution is then divided into two streams: one stream passes through a hydro-turbine to generate electricity, and the other goes through a pressure exchanger to assist in pressuring the inlet draw solution [29].

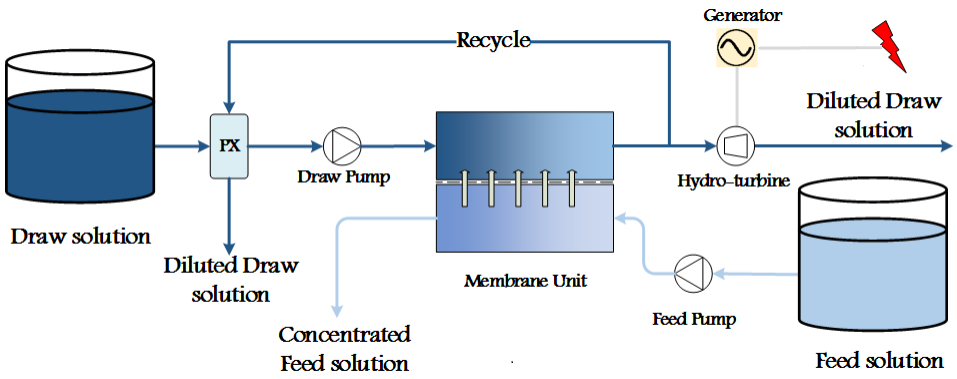


Figure 2.3: Schematic presentation of pressure retarded osmosis

### *2.2.2 Reverse electrodialysis (RED)*

RED is also a membrane-based technology, which uses the electrochemical potential difference for electrical power generation. Unlike PRO, RED uses multiple ions-selective membranes instead of single semi-permeable membrane [7]. In RED, two electrodes (a cathode and an anode) are placed in a cell, and a variable number of alternating anion and cation exchange membranes are stacked between these electrodes (Figure 2.4). The sections between the membranes are alternately fed with two solutions of different salinities. When an ion exchange membrane sepa-

rates two solutions of various salinities, the ions diffuse from higher concentration compartment to lower concentration compartment due to concentration difference. Therefore, cations diffuse through the cation exchange membranes (CEM) and anions diffuse through the anion exchange membrane (AEM), thus building up a positive potential on the cathode and negative potential on the anode, respectively [30]. As a result, a voltage difference occurs between the electrodes. When a load connected to these electrodes by an external circuit, electricity moves from the cathode to anode.

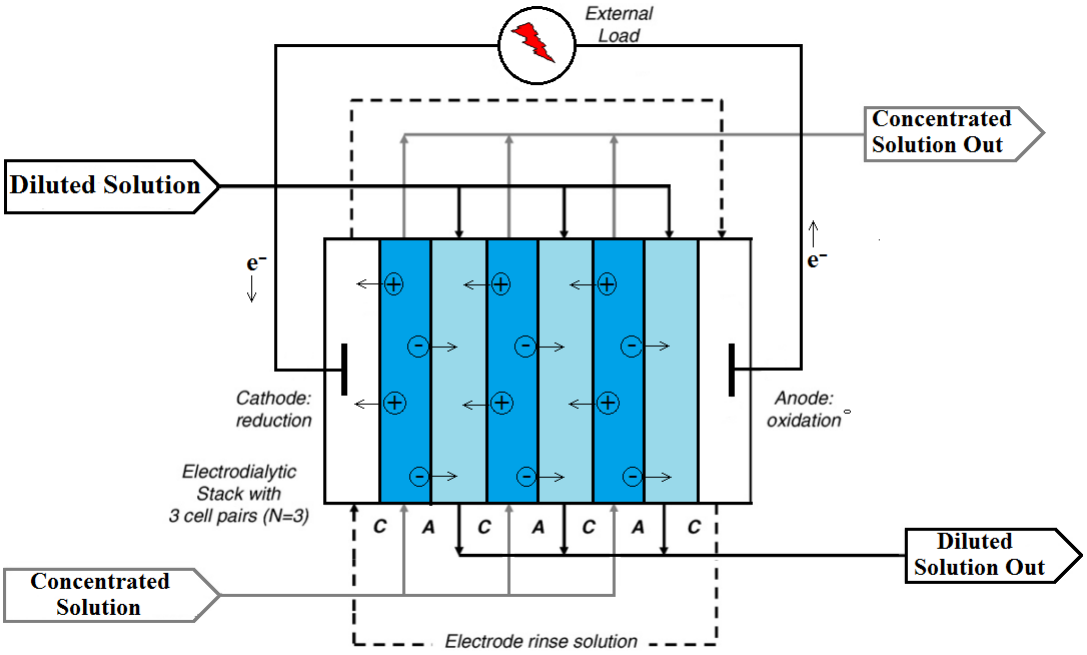


Figure 2.4: Schematic presentation of RED based on NaCl solutions [27]

### *2.2.3 Capacitive mixing (CAPMIX)*

CAPMIX is an electrochemical technology that directly converts salinity gradient energy to electrical energy by controlled mixing of two solutions. [11, 31, 32]. In

contrast with RED, in which the solutions simultaneously flow through different compartments of the cell, in CAPMIX the whole cell is sequentially filled with the two different salinity solutions. Electricity in a CAPMIX process is harvested using a four-step cycle, in which the cell is alternatively charged and discharged with solutions of different salinities (Figure 2.5).

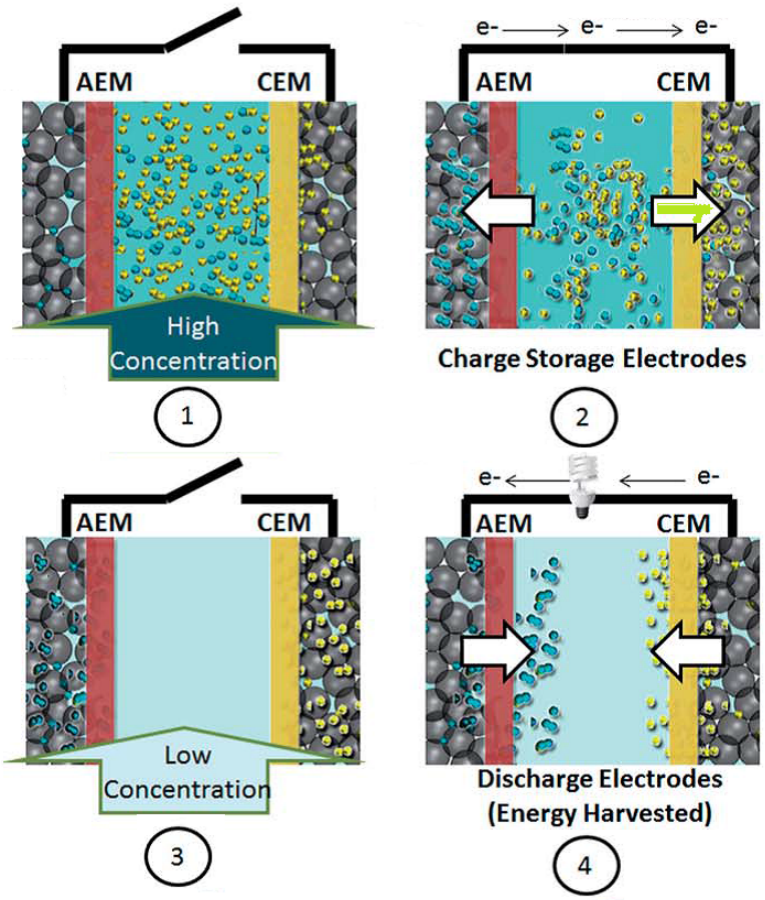


Figure 2.5: Schematic presentation of capacitive mixing [12]

In CAPMIX process, at first cell is filled with the high salt-concentrated solution and two electrodes (one positive and one negative) are immersed into the solution.

Then, the solution is charged by an external voltage source, thus increasing the charge on the electrodes but lowering the cell voltage (steps 1 and 2). Then, the external voltage is removed, and the high salt-concentrated solution is replaced by low salt-concentrated solution, which increases the cell voltage (steps 3 and 4). Due to the increase in cell voltage, current is discharged through a load and flows in the opposite direction of step 2. By the continuous rise and fall of cell voltage upon changing the solution, more energy can be captured in the low concentration solution than the energy used for charging the high salt-concentrated solution.

# 3. PRESSURE RETARDED OSMOSIS

This chapter explains the practical PRO process and development of equations to estimate the water and salt fluxes across the membrane. It also discusses the effects of concentration polarization, fouling of membrane, and reverse salt flux across the membrane for the development of flux equations. At the end of this chapter, it shows different models used to calculate water and salt fluxes.

## 3.1 Water and salt flux across a PRO membrane

### *3.1.1 Fluxes across ideal membrane*

Theoretically, an ideal PRO membrane only permits water to pass but no salts or ions cannot transfer through the membrane. In addition, for an ideal membrane, the water flux across the membrane, $J_W$ is a function of water permeability coefficient ($A$), the differential bulk osmotic pressure difference ($\Delta\pi_b$), and the differential hydraulic pressure ($\Delta P$), which is shown as follows [33]:

$$J_W = A(\Delta\pi_b - \Delta P) = A(\pi_{D,b} - \pi_{F,b} - \Delta P) \tag{3.1}$$

where, $\pi_{D,b}$ and $\pi_{F,b}$ refer to the bulk osmotic pressure of draw and feed solutions, respectively. Equation Equation 3.1 is only valid for perfectly selective membrane, while the bulk concentration is equal to the concentration at the membrane surface.

### *3.1.2 Fluxes across realistic membrane*

In practice, it is very difficult to find a perfectly semipermeable membrane. A small amount of salts or ions permeates through the membrane from concentrated solution to diluted solution due to the concentration gradients across the membrane. Figure 3.1 represents a concentration profile of a PRO membrane at steady state

condition. In the figures, three phenomena are mentioned that are responsible to reduce the water flux across the membrane:

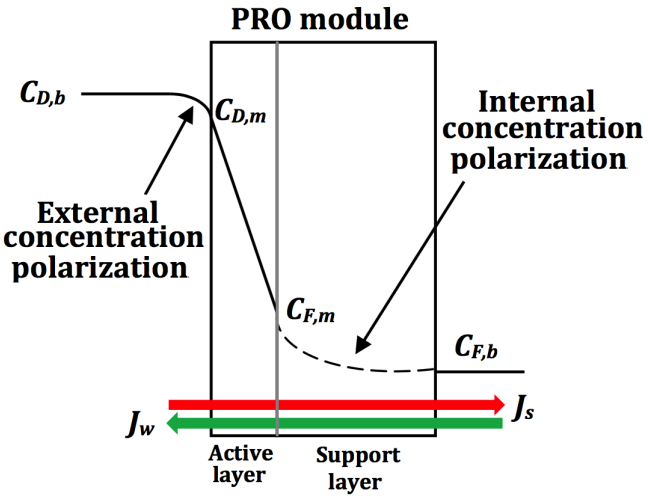


Figure 3.1: Concentration profile of a PRO module at steady state condition

- *Internal concentration polarization* $(ICP)$ : ICP occurs inside the porous support layer of the membrane, increasing the salt concentration at the interface of the active and support layers, from $C_{F,b}$ to $C_{F,m}$ (Figure 3.1). It detrimentally enhances the osmotic pressure of feed solution ($\pi_{F,m}$) by increasing the salt concentration at the active-support layers interface, which reduces the trans-membrane driving force.

- *External concentration polarization* $(ECP)$ : ECP takes place in the mass transfer boundary layer of the draw solution, reducing the salt concentration at the active later, from $C_{D,b}$to $C_{D,m}$ (Figure 3.1), which lowers the osmotic pressure of draw solution ($\pi_{D,m}$) at the active layer surface.

- *Reverse salt flux* : The membrane is no longer perfectly selective, reverse salt flux takes place due to uncontrolled mixing of solutions, which reduces the energy recovery in the process.

As consequences of these effects, mass transfer kinetics of water across the semipermeable membrane under applied hydraulic pressure, $\Delta P$ is more precisely described as:

$$J_W = A(\Delta\pi_m - \Delta P) = A(\pi_{D,m} - \Delta\pi_{F,m} - \Delta P) \tag{3.2}$$

The reverse salt flux across the membrane ($J_S$) is expressed as [16]:

$$J_S = B(C_{D,m} - C_{F,m}) \tag{3.3}$$

where, $B$ represents the salt permeability coefficient and $C_{D,m}$ and $C_{F,m}$ are the salt concentrations at the interface of the active and support layers, respectively. Lee et al. [33] conducted RO experiments to obtain the salt permeability coefficient and developed following correlation:

$$B = \frac{A(1 - R_S)(\Delta\pi - \Delta P)}{R_S} \tag{3.4}$$

where $R_S$ is the salt rejection coefficient defined as:

$$R_S = 1 - \frac{C_P}{C_F} \tag{3.5}$$

where, $C_P$ and $C_F$ are the salt concentrations of permeate solution and feed solution, respectively.

### *3.1.3 Power density of PRO process*

In PRO, the term 'power density' ($W$) is defined as the net power output per unit of membrane area. Mathematically, it is expressed as the product of water flux and differential hydraulic pressure across the membrane as follows:

$$W = J_W \Delta P = A(\Delta\pi - \Delta P)\Delta P \tag{3.6}$$

To obtain the maximum power density of PRO process, differentiate Eq.5.18 with respect to $\Delta P$ assuming $A$ as a constant:

$$\frac{dW}{d(\Delta P)} = A(\Delta\pi - 2\Delta P) \tag{3.7}$$

At maximum power density, $\frac{dW}{d(\Delta P)} = 0$; and $\Delta P = \frac{\Delta\pi}{2}$. By substituting the value of $\Delta P$ in Eq.5.18 yields:

$$W_{max} = A\,\frac{\Delta\pi^2}{4} \tag{3.8}$$

## 3.2 Concentration polarization

Concentration polarization (CP) is a phenomenon that reduces the effective osmotic pressure difference across the membrane. Mehta and Loeb [34, 35], and Lee et al. [33] introduced CP for PRO processes when they obtained their experimental outputs far lower than the outputs estimated based on theoretical osmotic pressure differentials. These researchers concluded that CP occurs on both sides of the membrane in two different ways: externally, on the dense layer side (active layer of the membrane) and internally, in the porous support layer. In PRO applications, the active layer of membrane faces the draw solution and the porous support layer faces the feed solution.

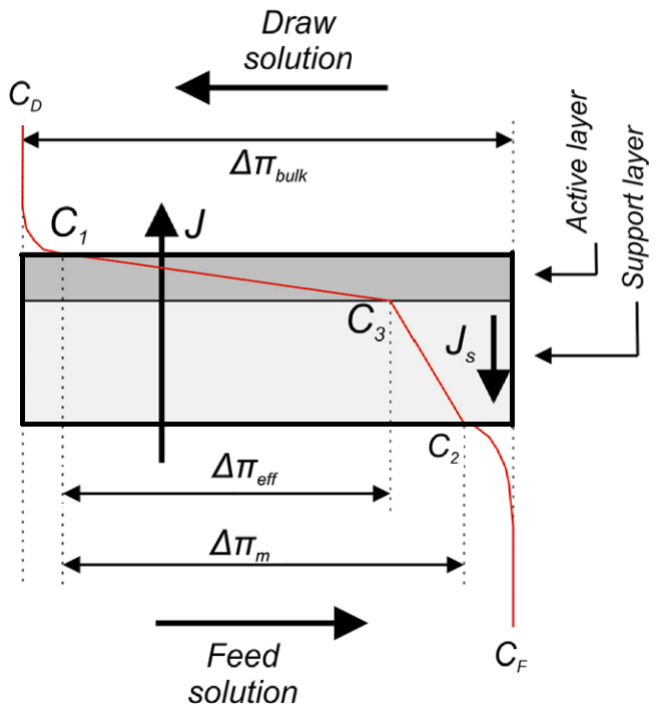


Figure 3.2: Illustration of concentration polarization on a PRO membrane [26]

External concentration polarization (ECP) is the depletion of salts that occurs over time on the outer surface of the membrane ($C_1$ and $C_2$ in Fig. 3.2), while internal concentration polarization (ICP) is referred to as the accumulation of salts within the porous support layer of the membrane ($C_3$ in Fig. 3.2). Recent studies have confirmed that ICP is more severe than ECP for PRO membrane, because the salts easily flows into the porous support layer since it has difficulty to penetrate the active layer [36–38]. It was reported that both ICP and ECP decrease the effective osmotic pressure differential, which drives the fluxes of water across the membrane, and finally reduces its power efficiency [34, 35]. This means that, instead of being

driven by the bulk osmotic pressure differential between $C_D$ and $C_F$, the water flux is actually driven by the osmotic pressure differential due to $C_1$ and $C_3$.

## 3.3 Historical development of PRO technology

Nowadays, pressure retarded osmosis is a very promising technology to recover osmotic energy from the mixture of saline solutions, although this concept was first reported in a Nature article by Pattle in 1954 [13]. In this article, Pattle demonstrated the possibility to use osmotic forces and selectively permeable membranes to obtain energy by mixing seawater and freshwater. According to Pattle, when a volume ($V$) of fresh water mixes with a much higher volume of seawater of osmotic pressure ($\pi$), the free energy released from the mixture is equal to $\pi V$. However, his research did not receive much attention in that time due to the abundance of fossil fuels. After the oil crisis in 1973, the subject of renewable energies gained importance, and PRO concept has received spasmodic attention, mainly in the form of design and economic viability evaluations [29, 33].

In 1974, Norman et al. [39] proposed a schematic diagram of an osmotic salination energy converter, from chemical potential to hydrostatic potential. In their design, they suggested that after water permeated across a semipermeable membrane from the freshwater chamber into a pressurized seawater chamber, the spill over water would turn a water wheel to power a generator. One year later, Loeb and Norman [40] successfully conducted some experiments and proposed the term PRO as a technology for harvesting energy by the mixing of two solutions of different salinities. In 1976, Loeb et. al. [14] successfully validated the principle of PRO technology and published first experimental PRO results, although the performance was not satisfactory due to the unusal behavior of membrane.

Although Loeb et al. [14] successfully explained the PRO technology, the power

obtained (from $1.56W$ to $3.27W$ for per $m^2$ membrane area using hyper-saline draw solution) from the experiments were far below the expected results based on the osmotic pressure difference across the membrane. In 1978, Loeb and Mehta [34] identified that 'internal concentration polarization' (ICP) has a strong adverse effect on the water permeation rate, which reduced the power generation by PRO [35]. In 1981, Lee et al. [33] found that concentration polarization occurs both internally and externally and reduce the effective osmotic pressure difference across the membrane. Lee et al. developed a model that only considers the effects of internal concentration polarization, which was used as the reference for further developments.

Based on Lee's consideration, Loeb et al. [41] successfully conducted several experiments on different PRO configurations to estimate theoretical mechanical efficiency, concluding that counter-current PRO configuration shows higher efficiencies. At the same time, Reali et al. [42] studied about the membrane behavior at different salt concentrations and computed the profile of salt concentration in the porous support layer in PRO systems, showing the effect of membrane characteristics, such as the water permeability coefficient $A$, the salt permeation coefficient $B$, the effective salt diffusivity $D$ and the support layer thickness $t_S$, on the water and salt permeation flux through an anisotropic membrane.

At the beginning of the 2000s, Loeb [43] continued his investigations on PRO applications for higher salinity water sources (e.g., Great Salt Lake). Later, the pressure exchanger device (originally developed for RO applications) was introduced to reduce internal power consumption, providing a cost-effective PRO system in 2002 [44]. After that, researchers have been continuously working on PRO to improve its performance. Many experiments and models have been proposed over time, but research has gained new impetus with the opening of the first PRO prototype power plant in 2009 by Starkraft, a Norwegian state-owned power company. The plant

was disconnected after the years of starting due to the insufficient power production. Starkraft reported that reverse salt fluxes across the membrane and fouling of the membrane along with concentration polarizations were the main reasons for that unfeasible power production.

Achilli et al. [38] expanded on the model developed by Lee et al. [33] by considering the external concentration polarization in an experimental and theoretical investigation of PRO systems: power density that exceeded 5.1 $Wm^{-2}$ was observed with a flat sheet cellulose triacetate (CTA) FO membrane. In 2011, Yip et al. [16] first introduced reverse salt fluxes and fouling of the membrane in their model to accurately determine the power density of PRO process. Experimental results lead to a projected peak power density of 6.1 $Wm^{-2}$. Since that time, several investigations have been published studying how to optimize PRO power density [38,45–47]. Many researchers are now developing the process and improving its performance [23,48,49].

## 3.4 PRO Model developments

### *3.4.1 Loeb model for water flux*

In 1976, Loeb [14] developed the first PRO model to estimate the water flux ($J_W$)across the membrane. Loeb expressed the water flux as a function of concentration and concentration gradient. In this model, he assumed that the salt salt flux ($J_S$)across the membrane is negligible, there is no ECP, and the concentration of the solution is proportional to the osmotic pressure of the solution. Based on the above assumptions, Loeb developed the following equation to estimate water flux ($J_W$):

$$J_W = A(\pi_D - \pi_F \; exp \; \frac{\Delta x}{D_{sp}} - \Delta P) \tag{3.9}$$

where $\pi_D$ and $\pi_F$ represent the bulk osmotic pressure of the draw and feed solution, respectively, $\Delta x$ is the thickness of the membrane and $D_{sp}$ is the diffusion coefficient

in the support layer.

### *3.4.2 Lee model*

In 1981, Lee et al. [33] developed a PRO model, where they effectively implemented the internal concentration polarization to estimate the water flux across the membrane. They also assumed that the effects of ECP is negligible. The equation derived by Lee et al. [33] to estimate the water flux as follows:

$$J_W = A\left(\pi_{D,m}\ \frac{1-\frac{C_{F,b}}{C_{D,m}}\ exp(J_W K)}{1+\frac{B}{J_W}\ [exp(J_W K)-1]} - \Delta P\right) \tag{3.10}$$

where $\pi_{D,m}$ is the osmotic pressure of draw solution at the membrane surface. $C_{F,b}$ and $C_{D,m}$ refer to the bulk concentration of feed solution and the concentration of the draw solution at the surface of the membrane, respectively, and $K$ is the solute resistivity.

### *3.4.3 Achilli model*

Achilli et al. [38] reworked on Lee's model and studied the effects of ECP on the water flux. They extended the Lee's model equation by implementing ECP. The equation developed by Achilli et al. [38] is as follows:

$$J_W = A\left(\pi_{D,b}\ exp\left(-\frac{J_W}{k}\right)\ \frac{1-\frac{\pi_{F,b}}{\pi_{D,b}}\ exp\left(J_W K\right)\ exp\left(-\frac{J_W}{k}\right)}{1+\frac{B}{J_W}\ [exp(J_W K)-1]} - \Delta P\right) \tag{3.11}$$

where $k$ is the mass transfer coefficient.

### *3.4.4 Yip model*

For last few decades, researchers developed many PRO models to ensure accurate estimation of water flux across the membrane. However, these models did not

consider the effects of reverse salt flux across the membrane. In 2011, Yip et al. [16] modified the Lee model by incorporating the effects of CP and reverse salt flux across the membrane. They assumed that the osmotic pressure is linearly proportional to the salt concentration. Yip's model equation to estimate the water flux is:

$$J_W = A\left(\frac{\pi_{D,b}\ exp\left(-\frac{J_W}{k}\right) - \pi_{F,b}\ exp(J_W K)}{1 + \frac{B}{J_W}\left[exp(J_W K) - exp\left(-\frac{J_W}{k}\right)\right]} - \Delta P\right) \tag{3.12}$$

where $\pi_{D,b}$ and $\pi_{F,b}$ represent the bulk osmotic pressure of the draw and feed solution, respectively, and $k$ is the mass transfer coefficient in the draw water side. The term $exp(-\frac{J_W}{k})$ demonstrate the effects of the external concentration polarization. The effect of the reverse permeation of the salt gave the denominator of Eq.3.12. Straub et al. [22] also developed another equation to estimate the salt flux across the membrane, which is given by:

$$J_S = B\left(\frac{C_{D,b}\ exp\left(-\frac{J_W}{k}\right) - C_{F,b}\ (J_W K)}{1 + \frac{B}{J_W}\left[exp(J_W K) - exp\left(-\frac{J_W}{k}\right)\right]}\right) \tag{3.13}$$

# 4. THERMODYNAMIC MODELS FOR ELECTROLYTE SOLUTIONS

One of the major objectives of this research is to determine the power densities of a PRO process. Various thermodynamic properties such as Gibbs free energy, osmotic coefficient, liquid density, enthalpy, and entropy are needed in order to calculate power densities accurately. To estimate all these properties, it is important to introduce an effective thermodynamic model for the electrolyte solutions. To develop such model, two different interactions: long range interactions between ion species and short range interactions between molecule-molecule, ion-molecule, and ion-ion should be taken into account. The relative importance of each type depends on the concentration of salts. This chapter mainly focuses on the Q-electrolattice EOS [50], and its scopes and limitations to predict different thermodynamic properties for PRO calculations. Additionally, some previous models for electrolyte solutions and their shortcomings are analyzed.

## 4.1 Debye-Hückel theory (D-H theory)

In 1923, Debye and Hückel [51] first developed a thermodynamic model for completely dissociated electrolyte system, which is considered to be one of the fundamental theories for estimating various thermodynamic properties of electrolyte solutions. This model is strictly applicable to very low concentration of electrolyte in water. It is also referred to as the ion-cloud model because the ions are considered to be distributed in a continuous dielectric media. The assumptions to develop this model are as follows:

1. The theory is only valid for solutions of charged ions (only anions and cations exist in the solution)

2. Only long-range interaction between ion species are considered in the development of this theory. The short-range interactions between water molecules and ionic species are ignored.

3. The solvent molecules only play the role to estimate ion-ion interactions because of its relative permittivity (dielectric constant) and its density.

4. The ions are not uniformly distributed throughout the solution. A positive or negative ion species is surrounded by a cloud of opposite ions. The charge of the cloud of ions contributes a total charge equal to that of the central ion but of opposite sign. Thus the solution is considered as a collection of central ions with their respective ion clouds.

5. The distribution function for the ion cloud around the central ion is assumed to be a Boltzmann distribution.

## 4.2 The Born equation

Although the Debye-Hückel model is a great invention to estimate various thermodynamic properties of electrolyte solutions, it only deals with the long range ion-ion interaction. Born [52] derived an equation to estimate the short range interaction force between an ion and the surrounding solvent molecules, which is known as solvation energy. In the electrolyte solution, an electric field is created around the charge that effects the polar molecules and redirect themselves to have as low energy as possible in the field. Born assumed that the ions are spherical with radius $r_i$ and charge $z_i$, and the charge is dissolved into a continuous dielectric solvent medium (see Figure 4.1). It is also assumed that all interactions are electrostatic in nature and there is no chemical interaction.

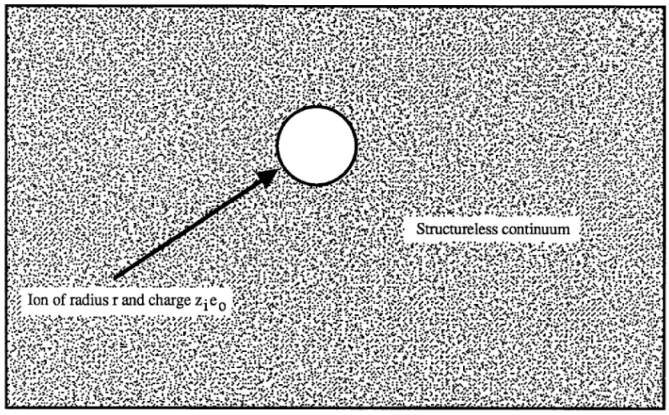


Figure 4.1: The basic assumption of the Born equation: Ion is spherical and floated in a continuous dielectric solvent medium [52]

When a charged ion moves from vacuum to a dielectric medium, the net work done to transfer ion into the medium is equal to the solvation energy. Born calculated this solvation energy of ion by integrating the electrostatic potential energy from the surface of the ion to infinity. The expression of the electrostatic contribution to the Helmholtz energy for a single ion system is as follows:

$$A = \frac{Z_i^2 e^2}{8\pi\epsilon r_i} \tag{4.1}$$

where $A$ is the Helmholtz energy, $Z$ is the ion charge, $r$ is the separation distance, and $e$ is the elementary charge of the electron ($1.6022 \times 10^{-19} C$). $\epsilon$ represents the permittivity of solvent, which is defined as the product of relative permittivity of the solvent and the permittivity of vacuum:

$$\epsilon = \epsilon_0 \epsilon_r \tag{4.2}$$

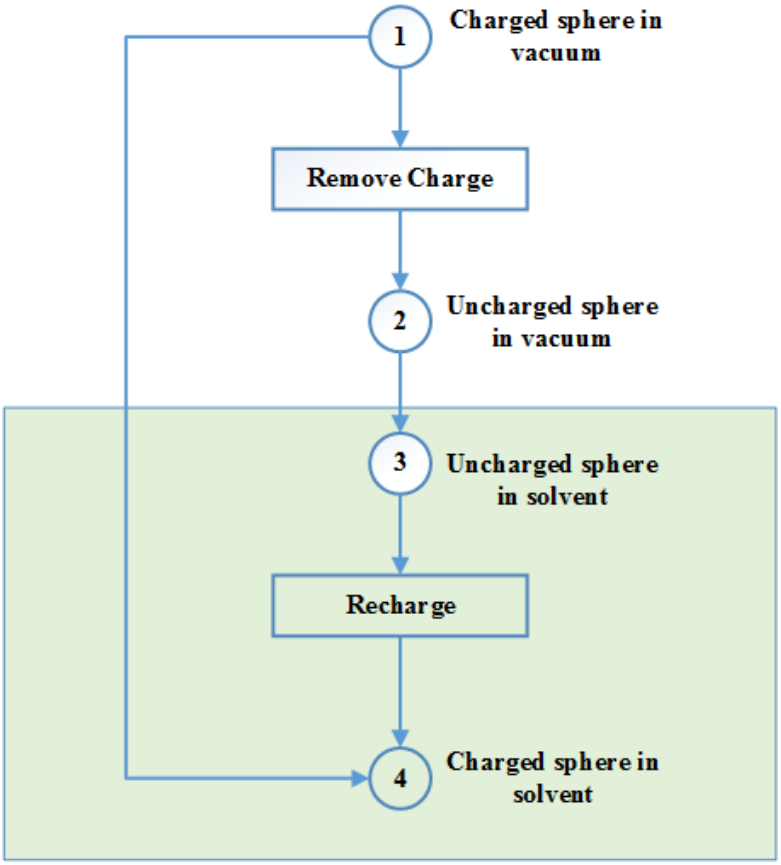


Figure 4.2: The thermodynamic path of the Born model [52]

In the Born model, the transfer of an ion from vacuum to a structureless continuum follows a thermodynamic path (see Fig. 4.2). Initially the spherical charged ion is located in vacuum. Then, $W_d$ work is applied to the ion to remove the charge from it. Later, this uncharged ion is transported into the solvent medium. It is assumed that this transfer involves no work. Then, the ion is recharged inside the solvent and the work done in charging ($W_c$) is determined. Therefore, the net work done for both discharging and charging the ion is the interaction force between ion and solvent molecules.

## 4.3 The mean spherical approximation (MSA)

The mean spherical approximation (MSA) is a thermodynamic model for the Helmholtz free energy for electrolyte solution [53, 54]. Similarly to the Debye-Hückel model, the MSA model also deals with long range ion-ion interaction. Both Debye-Hückel model and MSA model provide similar results for variable temperature, pressure and volume conditions, but only MSA accurately works to estimate the change in the screening length. Zuckerman et al. [55] stated that "At a purely theoretical level, however, one cannot be content since, a priori, there seem no clear grounds for preferring the DH-based theories-apart from their more direct and intuitive physical interpretation-rather than the more modern (and fashionable) MSA-based theories which-since they entail the pair correlation functions and the Ornstein-Zernike (OZ) relation-give the impression of being more firmly rooted in statistical mechanics".

## 4.4 Mattedi–Tavares–Castier (MTC) model

Mattedi et al. [56] developed an equation of state that accounts for short range interactions. The MTC EOS is obtained based on van der Waals generalized theory [57]. Also, this EOS is used in three different forms: as a molecular model, as a conventional group-contribution model, and as a region-contribution model. When applied as a region-contribution model, the water molecule is split in a electron donor, electron acceptor and dispersion region, which enable the representation of hydrogen bonding.

## 4.5 Q-electrolattice equation of state

The Q-electrolattice is an ion-based equation of state (Q-electrolattice EOS) developed for electrolyte solution in order to accurately determine various thermodynamic properties such as osmotic coefficient, osmotic pressure, density, enthalpy

and entropy at different conditions of pressure, temperature and concentration [58]. It incorporates the Mean Spherical Approximation (MSA) and Born Equation to model electrostatic interactions and solvation effects respectively, with the Mattedi-Tavares-Castier (MTC) EOS to model short-range interactions. Therefore, the residual Helmholtz energy for forming an electrolyte solution is thus given by:

$$A(T,V,n) = A^{MTC}(T,V,n) + \Delta A^{Born}(T,V,n) + \Delta A^{MSA}(T,V,n) \qquad (4.3)$$

### *4.5.1 Development of Q-electrolattice EOS*

The Q-electrolattice EOS was developed using the methodology presented by Myers et al. [59] for the Helmholtz energy. The residual Helmholtz energy at a given temperature and volume is calculated by adding various contributions along the hypothetical path shown in Figure 4.3. These contributions consist of ion-solvent and solvent-solvent interaction over short ranges, solvation effects, and ion-ion interactions over long ranges. To reach the final state from a reference state Q-electrolattice EOS follows a four steps path [57], as follows

$Step - I$**:** It is assumed that a reference mixture consisting of charged ions and molecules is in a hypothetical ideal gas state at temperature T and volume V. In the first step, the charges on all ions are removed. The change in Helmholtz energy is accounted by the Born equation for ions in a vacuum, $\Delta A^{Born}_{disc}$

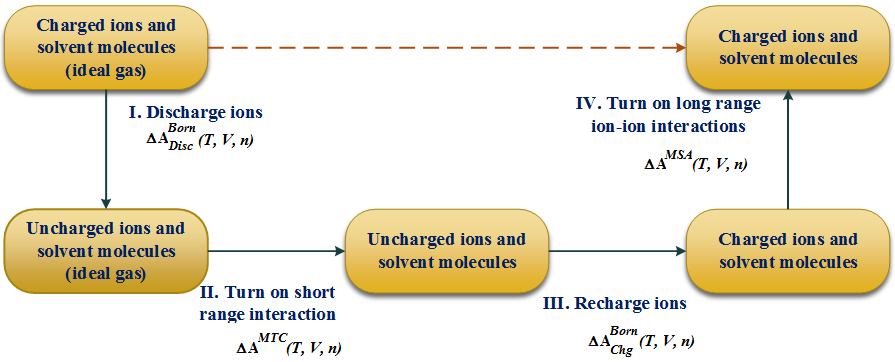


Figure 4.3: Path to the formation of an electrolyte solution at constant temperature and volume proposed by Myers et al. [59]

$Step - II$: The short-range attractive dispersion and repulsive forces due to excluded volume are turned on. Also, self-association of solvent molecules can occur. The MTC EOS is used to calculate the change in Helmholtz energy for this step, $\Delta A^{MTC}$.

$Step - III$: The ions are recharged. The change in Helmholtz energy is accounted for by the Born equation for ions in a dielectric solvent, $\Delta A^{Born}_{chg}$.

$Step - IV$: The long-range interactions among the ions in solution are taken into account using the Mean Spherical Approximation (MSA), and the corresponding change in the molar Helmholtz free energy is denoted by $\Delta A^{MSA}$.

As mentioned in Sec. 4.5, the Q-electrolattice EOS was developed for electrolyte solutions based on three different models: Born equation, Mean spherical approximation, and Mattedi–Tavares–Castier EOS. The Born equation contributes to estimate the change in Helmholtz energy to discharge an ion in vacuum (ideal gas) and recharging it in dielectric solvent medium. Therefore,

$$\Delta A^{B}(T,V,n) = \Delta A^{Born}_{chg}(T,V,n) + \Delta A^{Born}_{disc}(T,V,n) \tag{4.4}$$

On the other hand, the MSA term contributes to determining the variation of Helmholtz energy due to long-range electrostatic interaction between two ions in electrolyte solution. And, the MTC equation of state is used to estimate the short-range electrostatic interaction all pairs present in solution. According to the MTC EOS, the change of Helmholtz energy for ion-molecule interaction is expressed by following equation:

$$A^{MTC}(T,V,n) = A^{IGM}(T,V,n) + \Delta A^{MTC}(T,V,n) \tag{4.5}$$

So, from Eq. 4.3 we have,

$$A^{R}(T,V,n) = A(T,V,n) - A^{IGM}(T,V,n) = \Delta A^{MTC}(T,V,n) + \Delta A^{B}(T,V,n) + \Delta A^{MSA}(T,V,n) \tag{4.6}$$

The complete equations of the model are available in reference [50, 57, 58].

### *4.5.2 Assumptions of Q-electrolattice EOS*

In Q-electrolattice EOS, a single salt electrolyte solution is divided into five regions in order to model electrostatic interactions: three for solvent ($D$, $\alpha$, and, $\beta$), one for cation (C) and one for anion (A). To determine the MTC Helmholtz energy change, the model uses seven parameters to represent pure solvents. The model assumes that the region-region interaction (except for $\alpha$-$\beta$) are dispersion interactions, which are temperature dependent. In addition, it also assumed that the short-range interactions between the $\alpha$ and $\beta$ region are zero. In addition, hydrogen bonding interactions are taken to be temperature independent. This is summarized below:

$$\frac{u^{\alpha-\alpha}}{R} = \frac{u^{\beta-\beta}}{R} = \frac{u^{\alpha-D}}{R} = \frac{u^{\beta-D}}{R} = \frac{u^{D-D}}{R} \tag{4.7}$$

It is assumed that the interaction between the solvent and each charged species is equal; short-range interaction between opposite ions and same charge are neglected altogether. This is summarized below:

$$\frac{u^{\alpha-C}}{R} = \frac{u^{\beta-C}}{R} = \frac{u^{D-C}}{R} = \frac{u^{Solvent-C}}{R} \tag{4.8}$$

$$\frac{u^{\alpha-A}}{R} = \frac{u^{\beta-A}}{R} = \frac{u^{D-A}}{R} = \frac{u^{Solvent-A}}{R} \tag{4.9}$$

$$\frac{u^{A-A}}{R} = \frac{u^{C-C}}{R} = 0 \tag{4.10}$$

$$\frac{u^{A-C}}{R} = \frac{u^{C-A}}{R} = 0 \tag{4.11}$$

The parameters to determine mean ionic activity coefficient, and the values for surface area, volume and energy parameters for pure water are obtained using a set of equations derived by Zuber et al. (2014) [58] and Marcus (1988) [60].

### *4.5.3 Parameters*

Table 4.1 and Table 4.2 show the adjustable parameters for the Q-electrolattice EOS and interaction energy parameter for water respectively [58].

Table 4.1: Adjustable parameters for the Q-electrolattice EOS

| Cations | $u_0^{Solvent-ion}/R(K)$ | $\sigma_i(\dot{A})$ | Anions | $u_0^{Solvent-ion}/R(K)$ | $\sigma_i(\dot{A})$ |
|---|---|---|---|---|---|
| $H^+$ | -2216.0034 | 2.1538 | $F^-$ | -1931.0748 | 2.3005 |
| $Li^+$ | -2288.7600 | 1.8526 | $Cl^-$ | -1300.8669 | 2.3479 |
| $Na^+$ | -2022.9400 | 2.3222 | $Br^-$ | -1210.2382 | 2.9526 |
| $K^+$ | -1273.9691 | 3.4514 | $I^-$ | -1147.0504 | 3.6390 |
| $Rb^+$ | -299.2399 | 3.4996 | $OH^-$ | -1153.5526 | 0.9179 |
| $Cs^+$ | -207.3927 | 2.5493 | $NO_3^-$ | 3827.2756 | 3.6831 |
| $Mg^{2+}$ | -2793.9528 | 1.2572 | $ClO_3^-$ | -691.6599 | 2.7689 |
| $Ca^{2+}$ | -2235.5872 | 2.8218 | $ClO_4^-$ | -642.5937 | 3.8742 |
| $Sr^{2+}$ | -2145.3902 | 3.1060 | $SO_4^{2-}$ | 4435.7480 | 1.191 |
| $Ba^{2+}$ | -21082.6582 | 3.2000 | | | |

Table 4.2: Surface area, volume, and interaction energy parameters for water

| $Q^D$ | $Q^\alpha$ | $Q^\beta$ | r | $u_0^{D-D}/R$ (K) | $B^{D-D}/R$ (K) | $u_0^{\alpha-beta}/R$ (K) |
|---|---|---|---|---|---|---|
| 1.179308 | 0.830409 | 0.091808 | 2.141341 | -644.337 | 316.932 | -2892.937 |

# 5. MODEL FORMULATION AND SOLUTION METHODS

The ultimate goal of this thesis is to develop a model to determine the power density of a PRO process. This involves the solution of flux equations and the evaluation of several thermodynamic properties to estimate the power density accurately. This chapter mainly focuses on the formulation of a PRO model that can estimate the thermodynamic properties and calculate the power densities simultaneously. At the end of this chapter, it discusses the extension of this model from single-stage to two-stage membrane systems.

## 5.1 Model PRO process

This research work uses the exactly same process diagram that used in most of existing PRO studies. Figure 5.1 represents the schematic diagram of a PRO process with the assumptions made in this work.

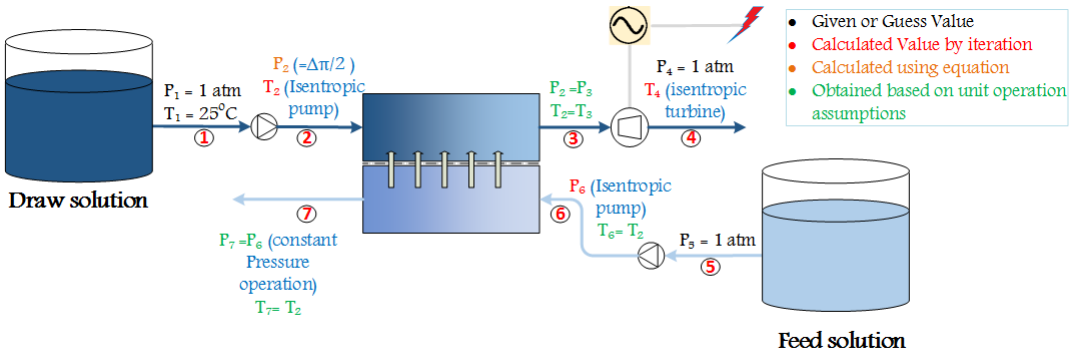


Figure 5.1: Schematic diagram of model PRO process

In this study, a concentrated draw solution of volume $V$ is pumped into the mem-

brane module at pressure $\frac{\Delta\pi}{2}$ (half of the initial osmotic pressure difference between draw and feed solutions). Simultaneously, a dilute feed solution enters to the other side of membrane module at atmospheric pressure. Due to the chemical potential difference a volume of water $\Delta V$ passes across the membrane from the diluted feed solution to the concentrated draw solution, thus diluting the draw solution and increasing the hydraulic pressure inside the draw compartment of membrane. The total volume of pressurized diluted draw solution $(\Delta V + V)$ passes through a hydroturbine to generate electricity. The net power for both studies were determined after deducting the power input to operate pump from the power harnessed by turbine.

### *5.1.1 Fundamental assumptions of the model*

To simplify the calculations, the following assumptions were made:

1. No pretreatment required for both feed and draw solutions.

2. No pressure drop inside the membrane. So, the hydraulic pressure of the input and output streams for each solution of membrane are equal. In this study, hydraulic pressure of the draw solution was maintained as half of the initial osmotic pressure difference, while the feed solution was at the pressure of 1 $bar$.

3. The temperature is constant throughout the membrane, which means all input and output streams of membrane have the same temperature.

4. Although all salts transfer across the membrane, only $NaCl$ is taken into account.

5. The operation of all rotating equipments (e.g., pumps and turbine) is adiabatic and reversible.

6. All units (e.g., pumps, turbine, and electricity generator) work with 100% efficiency, and there is no energy loss from the system.

## 5.2 Research procedure

Initially, an extensive literature survey was conducted on osmotic energy, available technologies to harness osmotic power from salinity gradient, PRO and its advantages over other technologies, and recently developed models and its limitations. To minimize the limitations of existing PRO models, this work developed a new model using Q-electrolattice EOS. The developed model is able to solve complex mass-transfer equations and to predict various thermodynamic properties simultaneously. The main procedures to achieve the goal of the research work were summarized as follows:

1. At first, the material balance calculations were done for each equipment to estimate the composition of each stream. The water and salt fluxes across the membrane were determined using Yip's model equation (Eq. 3.12 for water flux and Eq.3.13 for salt flux).

2. Calculated the osmotic pressure of both feed and draw solutions with respect to the freshwater.

3. Determined both ideal and residual entropy, enthalpy, and Gibbs free energy for each stream to predict actual entropy and enthalpy of the process.

4. Performed energy balance calculation and estimated the power inputs (for pumps) and outputs (for turbine). All input powers were considered positive while the output powers were negative.

5. The process was analyzed thermodynamically to estimate the maximum theoretical achievable energy in order to determine the process efficiency.

6. Compared the obtained results with literature experimental values to validate the developed model. Once the model verified, this model extended to multiple stage calculation. For validation calculation, the model used exactly same parameters and conditions that mentioned in the literature.

All these calculations were conducted using the Q-electrolattice EOS were implemented using the XSEOS tool [61], a thermodynamics computational package for Excel®. The solver tool in Excel® was utilized to simulate the process. A simplified algorithm for the PRO simulation is presented in Fig. 5.2, which was developed only for a single-stage membrane system. Additionally, in the algorithm, different colors were used for describing the operating conditions where blue color represents the initial guess value (or given value), red color indicates the calculated value, and black color used for normal process value. This algorithm was developed only for single–membrane PRO system, but is also applicable to multiple-membrane PRO system after small modifications.

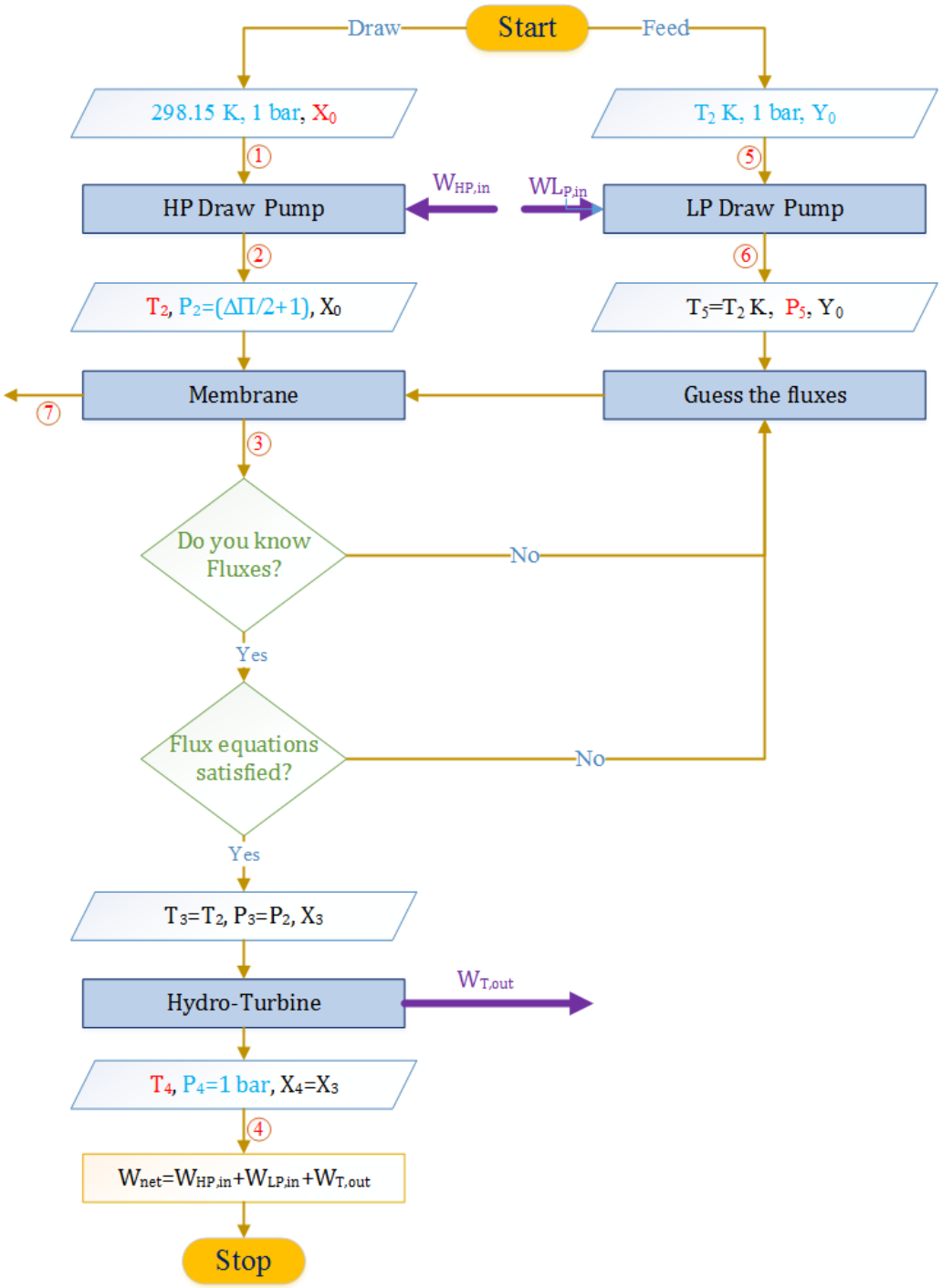


Figure 5.2: Model algorithm for single stage PRO process

### *5.2.1 Mass and energy balance*

The model developed in this thesis is very much temperature and composition sensitive. Therefore, the mass and energy balances play an important role for the accurate estimation of its outputs. This section discusses the essential assumptions and corresponding equations to conduct the mass and energy balance for each piece of equipment.

*Pump:*

Two pumps were used in this study: high pressure draw pump and low pressure feed pump (Fig.5.1). It was assumed that the both pumps are adiabatic and reversible, and operated at steady state conditions. For adiabatic and reversible operation-

$$\Delta S_{HP} = S_2(T_2, P_2) - S_1(T_1, P_1) = 0 \tag{5.1}$$

Here, $T_2$ is obtained by solving Eq.5.1, while $P_2 = \frac{\Delta\pi}{2}$ , and $T_1 = 298.15\ K$. On the other hand, for a steady state and isentropic pump, we know the following expression from the first law of thermodynamics:

$$W_{HP,in} = H_2(T_2, P_2) - H_1(T_1, P_1) \tag{5.2}$$

All the parameters in Eq.5.2 are known and thus give us the net work input to the pump.

*Membrane:*

Ideally, the membranes used in PRO studies are considered as perfectly semipermeable, and only allow water to transfer across them. However, in practice, the membranes are not perfectly selective and a small amount of salt passes through the membrane. This research accounts for both water and salt fluxes, which were

determined by using Yip's equations (Eq. 3.12 and Eq. 3.13). The magnitude of the parameters [water permeability coefficient ($A$), salt permeability coefficient ($B$), structural parameter ($S$), and mass transfer coefficient ($k$)] used in Yip's equations depend on the concentration of the solutions and the characteristics of the membrane. All numerical values for these parameters were taken from literature directly. Table 5.1 represents the list of parameters used in the simulation model to calculate water and salt fluxes. The mass balance equations for membrane are given by:

Table 5.1: Parameters used for modeling a PRO process

| Definition | Symbol | Unit | Value |
|---|---|---|---|
| Water permeability coefficient | A | $Lm^{-2}h^{-1}bar^{-1}$ | 0.673-1.23 |
| Salt permeability coefficient | B | $Lm^{-2}h^{-1}$ | 0.3996-2.62 |
| Structural parameter | S | $\mu m$ | 400-600 |
| Diffusion coefficient | D | $m^2s^{-1}$ | 1.485-1.566 |
| Mass transfer coefficient | k | $Lm^{-2}h^{-1}$ | 138.6-311.8 |
| Solute Resustivity | K | $sm^{-1}$ | $1.52\times10^5$ |

$$\dot{m}_{W,4} = \dot{m}_{W,3} + A^* \times J_W(T, P_4, \dot{m}_4, P_{10}, \dot{m}_{10}) \tag{5.3}$$

$$\dot{m}_{W,9} = \dot{m}_{W,10} + A^* \times J_W(T, P_4, \dot{m}_4, P_{10}, \dot{m}_{10}) \tag{5.4}$$

where, $A^*$ and $\dot{m}$ represent the area of membrane and mass flow rate respectively.

*Turbine:*

The assumptions and operating conditions for the turbine were considered the same as for the pumps. The only difference between them is that pump consumes energy whereas the turbine generates energy. The entropy equation for an isentropic turbine

is expressed as follows:

$$\Delta S_T = S_4(T_4, P_4) - S_3(T_3, P_3) = 0 \tag{5.5}$$

The solution of Eq.5.5 gives the value of $T_4$, while $P_3 = \frac{\Delta\pi}{2}$, $T_3 = T_2$, and $P_4 = 1\ bar$. At the steady state condition, the energy balance equation for isentropic turbine is written as follows:

$$W_T = \Delta H_T = H_4(T_4, P_4) - H_3(T_3, P_3) \tag{5.6}$$

### *5.2.2 Osmotic pressure calculation*

When a saline solution is separated from the pure water by a semipermeable membrane, water passes through the membrane to saline solution. Osmotic pressure is the minimum pressure applied to the pure water to resist the water transport across the membrane. Therefore, the osmotic pressure refers to the differential pressure between saline solution and the pure water when there is no flow across the membrane.

$$Osmotic\ pressure(\pi) = P_S - P_0 \tag{5.7}$$

where $P_s$ and $P_0$ represent the pressure of saline solution and the pure water respectively. In this work, it was assumed that the pressure of the pure water is 1 $bar$. If there is no water flow across the membrane, the chemical potential of water in the saline solution and in the pure water would be equal for a given temperature.

$$\mu_{water,s} = \mu_{water,0} \tag{5.8}$$

where,

$$\mu_{water,s} = \mu^{ig,pure} + RT\ ln\left(\frac{f_S}{P_0}\right) \tag{5.9}$$

$$\mu_{water,0} = \mu^{ig,pure} + RT\ ln\left(\frac{f_0}{P_0}\right) \tag{5.10}$$

In Eq.5.9 and Eq.5.10, $f_S$ and $f_0$ represent the fugacity of water in the saline solution and in the pure water, respectively. Also, $T$ is the absolute temperature and $R$ is the ideal gas constant ($8.314 Jmol^{-1}K^{-1}$). Substituting these equations into Eq. 5.8, thus gives the following condition:

$$f_S = f_0 \tag{5.11}$$

$$x_S\phi_S(T_S, P_S, x_S)P_S = x_0\phi_0(T_0, P_0, x_0)P_0 \tag{5.12}$$

where the subscript $S$ and 0 represnt the saline solution and pure water, respectively. In these equations, $x$ is the composition of water, $P$ is the pressure inside the compartment, and $T$ is the temperature. Therefore, in Eq.5.12, only $P_s$ is unknown. Solving Eq.5.7 and Eq.5.12 we can obtain the osmotic pressure of a saline solution.

### *5.2.3 Entropy and Enthalpy Calculation*

There is no experimental method available to measure the actual values of entropy and enthalpy directly. This work evaluates these properties using the concept of residual properties. The expressions for entropy ($S$) and enthalpy ($H$) for the actual system are written as follows:

$$H = H^{ig} + H^R \ and \ S = S^{ig} + S^R \tag{5.13}$$

where superscript $ig$ and $R$ represent the ideal-gas value and residual value respectively. General expression for $H^{ig}$ and $S^{ig}$ are given by:

$$H^{ig}(T,P) = H^{ig}_{ref}(T_{ref},P_{ref}) + \int_{T_{ref}}^{T} C^{ig}_{P}\ dT \tag{5.14}$$

$$S^{ig}(T,P) = S^{ig}_{ref}(T_{ref},P_{ref}) + \int_{T_{ref}}^{T} C^{ig}_{P}\ \frac{dT}{T} - R\ ln\left(\frac{P}{P_{ref}}\right) \tag{5.15}$$

In Eq.5.14 and Eq.5.15, $C_P$ denotes the specific heat capacity at constant pressure and the subscript 'ref' represents the reference state. 298.15 $K$ and 1 $bar$ are used as the reference state for this study. The residual enthalpy and entropy for this model have been estimated from excess Gibbs free energy at constant pressure and composition using Eq.5.16and Eq.5.17.

$$H^{R} = -RT^{2}\left[\frac{\delta\left(\frac{G^{R}}{RT}\right)}{\delta T}\right]_{x,P} = -RT^{2}\left(\frac{\Delta(\sum x\ ln\phi)}{\Delta T}\right) \tag{5.16}$$

$$S^{R} = \frac{\left(G^{R} - H^{R}\right)}{T} \tag{5.17}$$

### *5.2.4 Power density of PRO process*

The performance of a PRO process is analyzed based on the numerical value of power density, which is defined as the net power harnessed from salinity gradient for per $m^2$ of membrane area. In a PRO process, pumps consume electrical energy and the turbine harvests electrical or mechanical power. Therefore,

$$Power\ density = \frac{Total\ power\ generation - Total\ power\ consumption}{Total\ membrane\ area\ (m^2)} \tag{5.18}$$

## 5.3 Model extension

As mentioned earlier, most of the PRO works (both experimental and modeling) were conducted in a single-stage membrane system, which only considered $Na^+$ and $Cl^-$ ions, whereas, in practice, saline waters contain other ions in addition to these two. This work reports simulations of PRO processes that consider the presence of multiple ions in solution ($Na^+$, $Mg^{2+}$, $Ca^{2+}$, $K^+$, $Cl^-$, and $SO_4^{2-}$) and use a single thermodynamic model to evaluate all necessary physical properties. Finally, this work is implemented to a two-stage PRO system with three different configurations and compared with the single-stage PRO performance.

Three different configurations of two-stage PRO processes used in this study are shown in Figs. 5.3- 5.5. The only difference of these configurations was the position and the number of turbines used. In Fig.5.3, both the feed and draw solutions were connected in series, and the salinity gradient is continuously treated in two stages. The final stream of the draw solution is passed through a turbine. However, in Fig. 5.4 and Fig. 5.5, two individual turbines were used. In Fig. 5.5, the draw solution is first divided into two branches that flow separately into two stages. The excess volume of solution in the draw side of the first membrane passes through a turbine, and the remaining volume of solution enters in the second membrane as the new draw solution. In the case of Fig. 5.4, the outlet stream from the first membrane is passed through a turbine and entered as the new draw solution. And finally, the total solution is passed through another turbine.

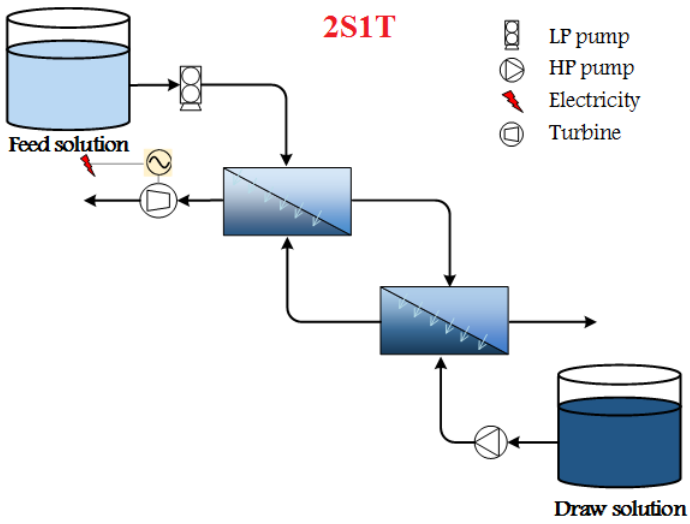


Figure 5.3: Schematic diagram of two-stage PRO process with a single turbine (2S1T)

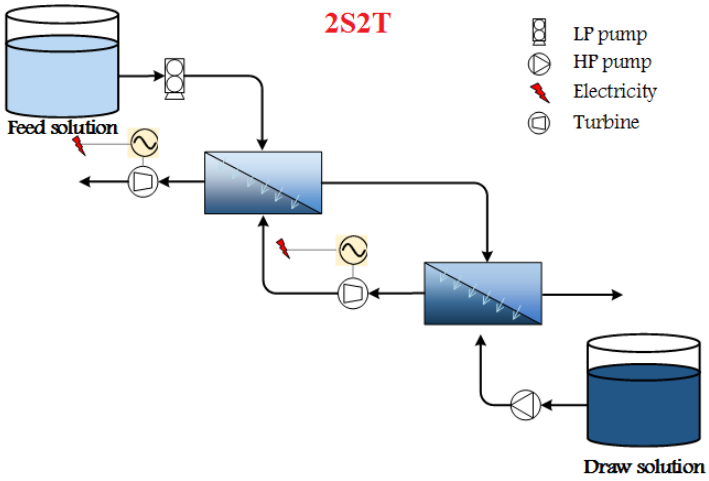


Figure 5.4: Schematic diagram of two-stage PRO process with a two turbine (2S2T), while the discharge of first turbine is the feed of second membrane

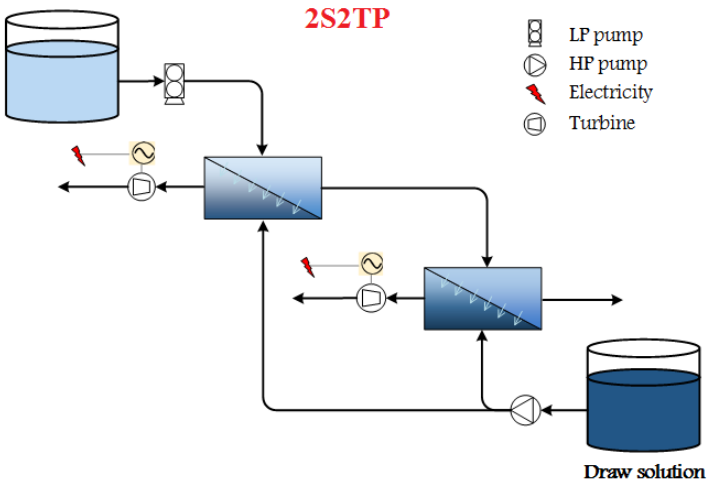


Figure 5.5: Schematic diagram of two-stage PRO process with a two turbine (2S2TP), while the discharge of first turbine divided into two parts: one passes through the turbine and another goes across the membrane

To evaluate all thermodynamic properties, and to calculate the water and salt fluxes across the membrane, and power density for the two-stage system, this model used exactly the same assumptions and methodology developed for the single-stage system.

# 6. RESULTS AND DISCUSSION

This chapter represents the results of the thesis. The contents of this chapter are divided into three sections: the first section represents the validation of the developed model whereas the second section studies the effects of various process variables, such as concentrations, flow rates, osmotic pressure difference, etc. on the power output of PRO. These two sections mainly focus on single-stage PRO system with only $Na^+$ and $Cl^-$ ions in both feed and draw solutions. The last section deals with the extension of the developed model for solutions of multiple ions and multiple stage membrane systems.

## 6.1 Model validation

Model validation illustrates how much a model represents the actual system. This work developed a single framework that can give three different outputs: osmotic pressure, water and salt fluxes across the membrane, and power density. To validate the developed model, all these outputs are compared with either experimental data or existing models. For validation, the developed model used exactly the same solution characteristics, model parameters, and the operating conditions that were mentioned in the literature. This section mainly discusses the comparison for model validation.

### *6.1.1 Osmotic pressure validation*

Osmotic pressure calculation is the most significant part of PRO studies because the mass transfer across the membrane and the power density are the function of the osmotic pressure difference. To ensure accurate estimation of osmotic pressure, the modeled results with the Q-electrolattice EOS were compared with the experimental results published by Hamdan et al. [62] who conducted their experiments to measure

the osmotic pressure for $NaCl$ and $MgCl_2$ solutions. The modeled results are also compared with the results obtained by OLI-analyzer, which is a computer-based software used to predict the chemical properties of electrolyte solutions. However, the main limitation of this analyzer is that it can only predict the chemical properties of an electrolyte solution at given temperature and pressure, but cannot determine the power density and the mass fluxes across the membrane.

Figures 6.1 and 6.2 represent the osmotic pressure as a function of concentration for $NaCl$ and $MgCl_2$ solutions, respectively. In both figures, the osmotic pressure calculated with Q-electrolattice EOS is very close to the experimentally measured osmotic pressure at low concentration, but for higher concentration, it deviates from the experimental results. The increase in deviations between calculated and experimental thermodynamic properties as salt concentrations increase is a feature common to practically all models for electrolyte solutions. The results of the Q-electrolattice EOS and of the OLI-analyzer are very similar.

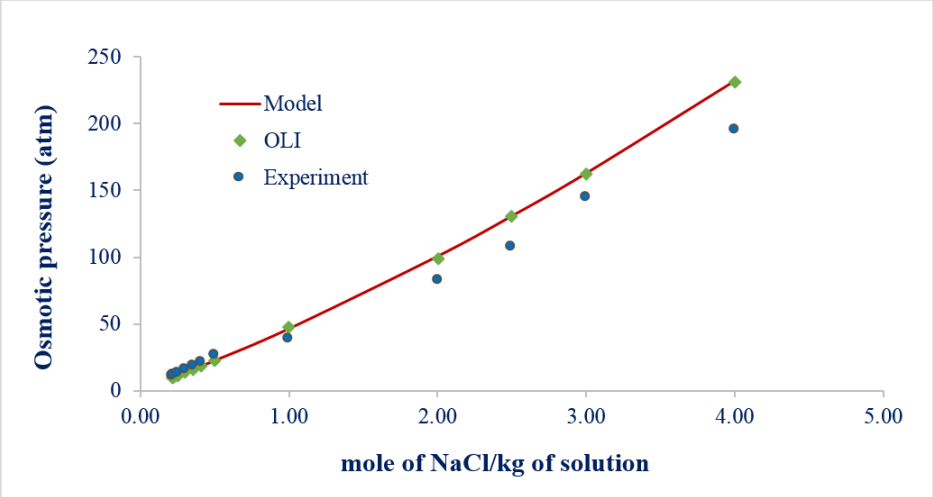


Figure 6.1: The comparison of modeled osmotic pressure with experimental data [62] and the results obtained by OLI-analyzer for $NaCl$ solution at $25^0C$ temperature.

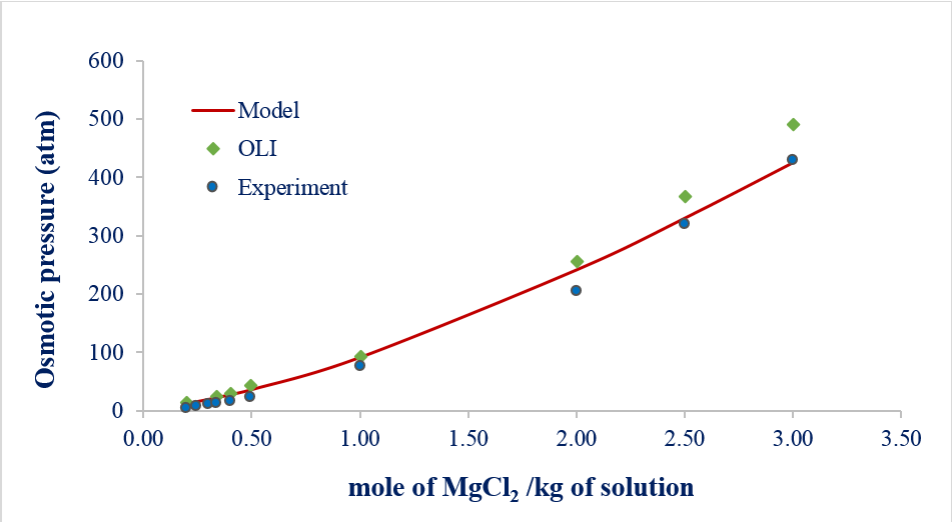


Figure 6.2: The comparison of modeled osmotic pressure with experimental data [62] and the results obtained by OLI-analyzer for $MgCl_2$ solution at $25^0C$ temperature.

### *6.1.2 Fluxes and power density validation*

In a PRO process, water flux plays the most important role in the power calculation (approximately, power is equal to the pressure difference across the turbine times the volumetric water flow rate). However, the determination of water flux across the membrane is the most arduous task of PRO studies, because the water flux is an implicit function. In this work, the modeled water flux and corresponding power density were compared with both literature experimental and model results published by Achilli et al. [38]. Figures 6.3(a) and 6.3(b) present the amount of water transport through the membrane and the power density as a function of applied pressure, respectively.

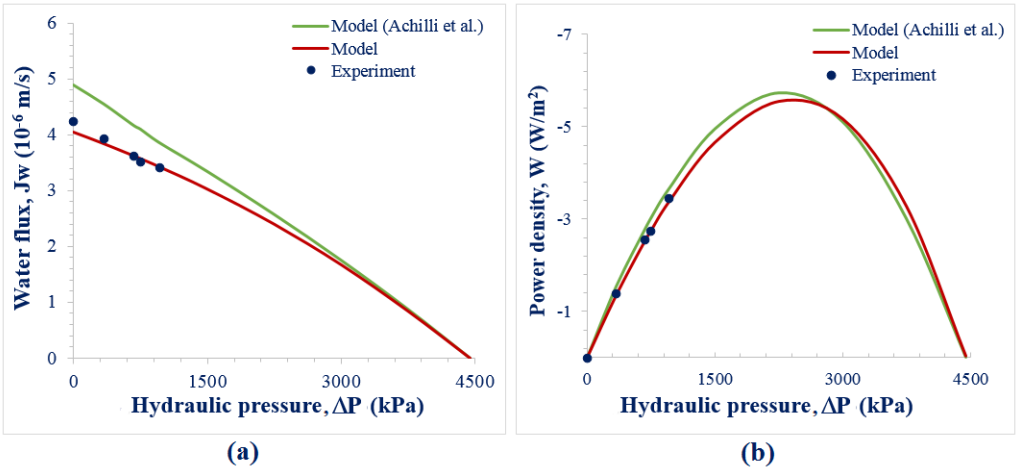


Figure 6.3: Modeled results of (a) power density, $W$ and (b) water flux, $J_W$ as a function of applied hydraulic pressure, $\Delta P$ compared with model and experimental results published by Achilli et al. [38].

Both figures show that the literature experimental results (solid blue dot) are very close to the results obtained by this work (solid red line), while the literature modeled results (solid green line) over estimate both of them. The main reason behind this overestimation is that Achilli et al. did not consider the reverse salt flux to calculate water flux and power density, which is taken into account in this work. The volume flow rates used for both feed and draw solutions were equal to $0.5L.min^{-1}$. This work further compared with the existing PRO model developed by Straub et al. [2], which uses the same equations and methodology to determine the power output, and water and salt flux across the membrane. Figure 6.4 demonstrates the trend of (a) power density and (b) water and salt fluxes across the membrane for various applied pressure. From the figure, it is clearly seen that the modeled results (solid line) are in excellent agreement with the literature model (rectangle dot).

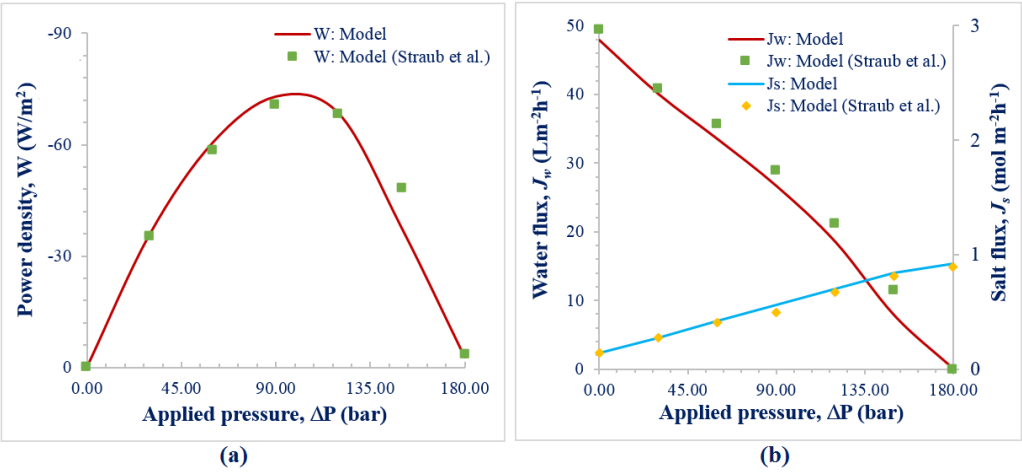


Figure 6.4: Modeled results of power density, $W$ as a function of applied hydraulic pressure, $\Delta P$ compared with an existing model developed by Straub et al. [2].

The previous comparisons between the modeled results and the literature data (both experimental and model) show that the model developed in this work can accurately determine the osmotic pressure, water, and salt fluxes across the membrane, and the power density.

## 6.2 Effects of model variables

The power density and mass flux across the membrane in PRO depend on various operating variables such as the concentration of draw and feed solutions, the osmotic pressure difference between the solutions, types of membrane and their area, membrane orientations, temperature, etc. This section mainly investigates the effects of the concentration of feed and draw solutions, osmotic pressure difference, and the area of the membrane on water and salt fluxes across the membrane and the power density.

### *6.2.1 Effects of the concentrations on power density*

The power density of a PRO process proportionally depends on the osmotic pressure difference ($\Delta\pi$) between the feed and draw solutions, while osmotic pressure is a function of the concentration of the solutions. Different concentrations of the feed and draw solution can be used in PRO studies to obtained sufficient $\Delta\pi$ in order to establish an economically feasible process. However, a PRO process does not become viable until it can recover more that $5Wm^{-2}$ power from the mixing of solutions **??**. Therefore, an accurate selection of the concentration of these two solutions is necessary to exceed this minimum limit of power density. The effects of the concentrations of both draw and feed solutions on power density were investigated in this research work. To analyze the effects of the concentrations on the power density, various combinations of feed and draw solutions were used [In this work, combinations of three feed solutions with different concentrations ($0.5M$, $0.75M$, and $1.0M$ of NaCl) and three different draw solutions ($3.0M$, $4.0M$, and $5.0M$ of NaCl) were used]. To reduce the number of simulation, when working with feed solutions the concentration of the draw solution was always $3.0M$, whereas, for draw solutions simulations, the feed solution was $1.0M$.

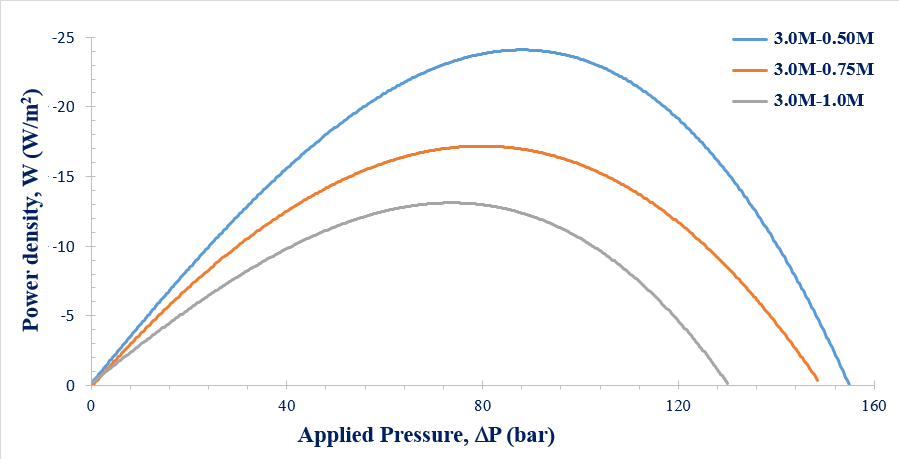


Figure 6.5: Effects of feed solution concentration on power density, $W$ in PRO. Model conditions: $3M$ NaCl draw solution, $T = 25^0C$, and flow rates of both feed and draw solutions are $1.0L.min^{-1}$.

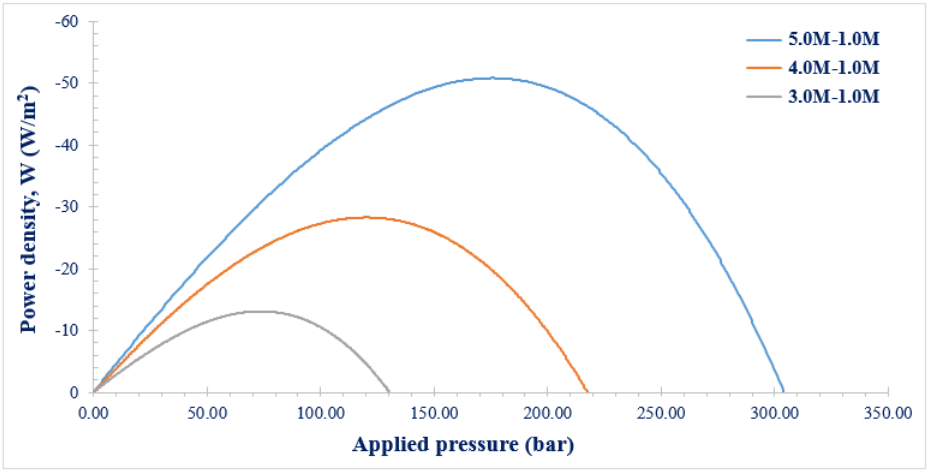


Figure 6.6: Effects of draw solution concentration on power density, $W$ in PRO. Model conditions: $1.0M$ NaCl feed solution, $T = 25^0C$, and flow rates of both feed and draw solutions are $1.0L.min^{-1}$.

In Fig. 6.5 and Fig. 6.6, the modeled power density is drawn as a function of applied hydraulic pressure difference between the solutions. As expected, the power density values increase as the concentration of the feed solution becomes lower. The power density reaches a minimum when the $\Delta P$ is close to the osmotic pressure difference. It is often stated in the literature that the maximum power density occurs when $\Delta P$ is half of the osmotic pressure difference. These figures show that under a less restrictive set of assumptions, the maximum power density occurs for slightly larger $\Delta P$ values. In addition, Fig 6.5 shows that decreasing the concentration of the feed solution leads to increase of the power density. On the other hand, Fig. 6.6 shows that the power density is significantly increases with increasing the concentration of the feed solution. Because, the osmotic pressure difference between the draw and feed solutions increases when the concentration of draw solution is increased.

### *6.2.2 Effect of the flow rates*

In this section, the effect of the flow rate is studied. The process was simulated under different flow rates ($0.5 L.min^{-1}$, 1.0 $L.min^{-1}$, and 2.0 $L.min^{-1}$). The feed flow rate was the same as the draw during all run of processes. The concentration of the draw solution was $3.0M$ whereas the concentration of the feed solution was $1.0M$. The modeled power density was calculated as shown in Fig. 6.7. Figure 6.7 shows that by increasing the operating flow rate, the energy increases remarkably. It can be seen also that the increase of the power density is quite important when the flow rate increases. This behavior can be explained according to film theory: when the flow increases, the thickness of the mass transfer boundary layer becomes thinner, which results in a higher rate of mass transfer across the membrane, and consequently, reduces the external concentration polarization.

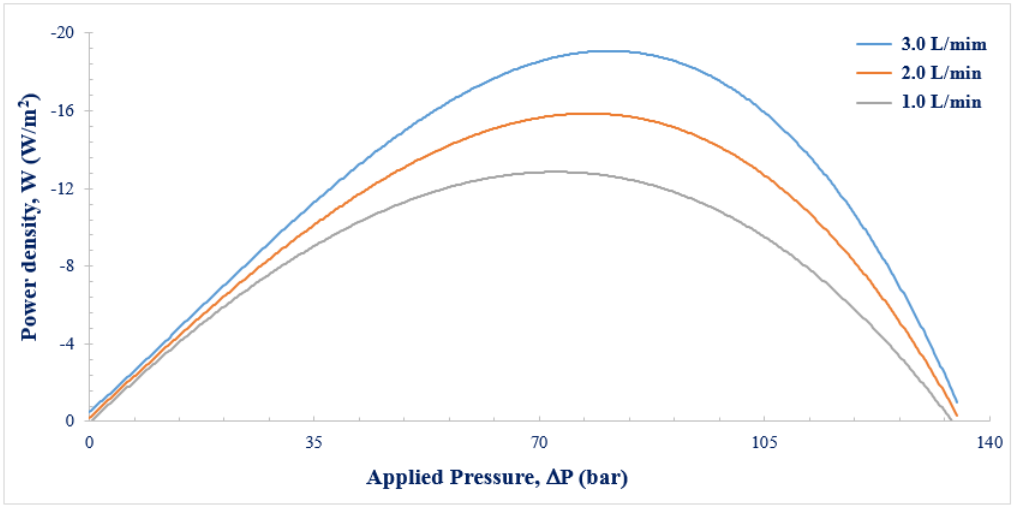


Figure 6.7: Modeled power density as a function of applied pressure for different flow rates. Model conditions: $1.0M$ NaCl feed solution, $3M$ NaCl draw solution, equal flow rates of draw and feed solution, and $T = 25^0C$

### *6.2.3 Effect of osmotic pressure difference on fluxes*

In PRO, water transfer across the membrane depends on the osmotic pressure difference between two solutions. In this section, the effects of osmotic pressure difference due to the concentration gradients are studied in order to determine the water and reverse salt flux across the membrane. As mentioned earlier that, osmotic pressure of a solution increases with increasing the concentration of the solution, thus increasing water permeation through the membrane. To investigate the effects of osmotic pressure difference, five feed solutions with different concentration (0.3, $0.6M$, $0.9M$, $1.2M$, and $1.5M$ of NaCl) were simulated against five different draw solutions (2.0, $3.0M$, $4.0M$, $5.0M$ and $6.0M$ of NaCl). To study the effects of feed concentrations, the draw solution was always $3.0M$, and for draw solution simulation, the concentration of feed solution was maintained as $1.0M$. For both of these studies,

the flow rates of both the draw and feed solutions were 1.0 $L.min^{-1}$.

To estimate the water and salt fluxes across the membrane, Yip's model equations were solved numerically for a range of concentration, keeping the values of all parameters. Figure 6.8 shows that the water flux across the membrane decreases with increasing the concentration of the feed solution. The concentration of the draw solution of this study was constant. When the concentration of feed solution increases, the osmotic pressure difference between the solutions decreases, thus reducing the water flux across the membrane and therefore, the power density. In addition, the salt flux across the membrane also decreases but slightly with increasing the feed concentration because salt flux is directly proportional to the water flux across the membrane. On the other hand, the osmotic pressure difference is increased with increasing the concentration of draw solution when the concentration of the feed solution is constant. Thus, the water and salt fluxes across the membrane, which leads to increase the power density of the process.

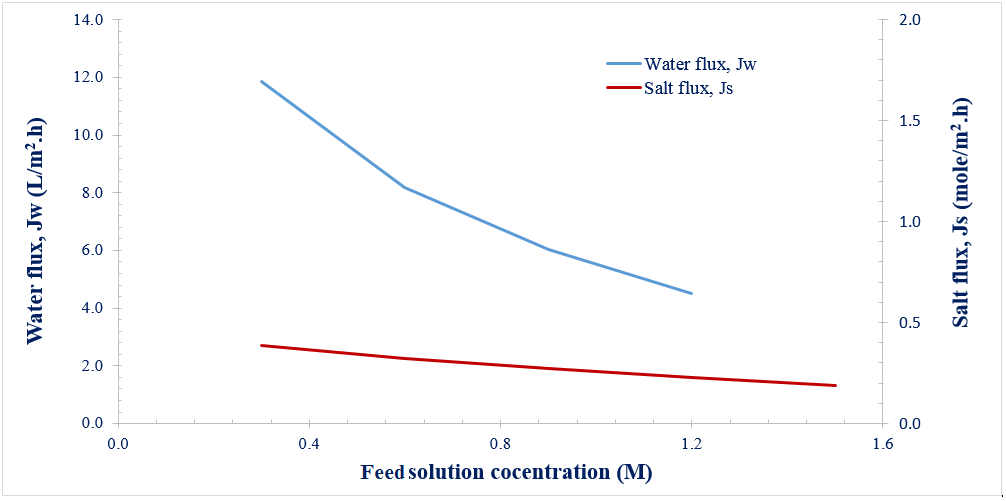


Figure 6.8: Effects of osmotic pressure difference (due to the change of the concentration of feed solution) on water and salt fluxes. Model conditions: $3.0M$ NaCl draw solution, $\Delta P = \Delta\pi/2$, $1.0L.min^{-1}$ flow rates for both solutions , and $T = 25^0C$

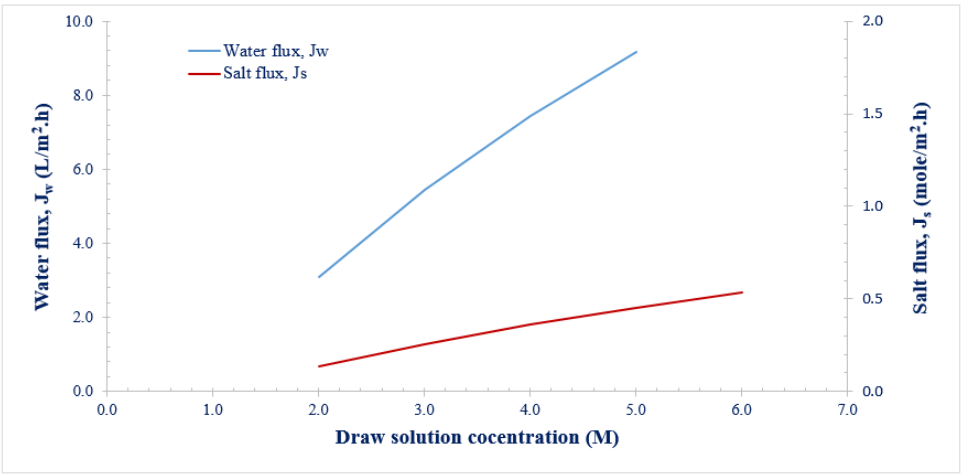


Figure 6.9: Effects of osmotic pressure difference (due to the change of the concentration of draw solution) on water and salt fluxes. Model conditions: $1.0M$ NaCl feed solution, $\Delta P = \Delta\pi/2$, $1.0L.min^{-1}$ flow rates for both solutions , and $T = 25^0C$

### *6.2.4 Effect of membrane area*

The membrane is the most important unit in PRO studies. The water transfer across the membrane depends on the types and area of the membrane as well as on the osmotic pressure difference. More membrane area allows more water to pass through it. Figure6.10 represents the power harvested by mixing of two solutions of different salt concentrations. It shows that the power output from a PRO process is proportional to the area of the membrane. However, the cost of a PRO membrane is very high compared to that of a RO membrane. Thus, a reasonable membrane area should be chosen in order to develop a feasible PRO process.

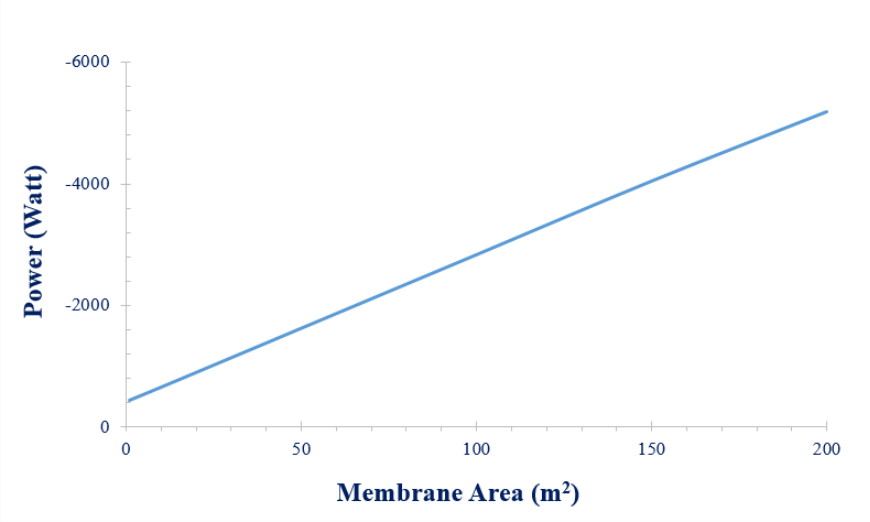


Figure 6.10: Effects of membrane area on power density, $W$ in PRO. Model conditions: $1.0M$ NaCl feed solution, $4.0M$ NaCl feed solution, both the feed and draw flow rates are $0.5m^3s^{-1}$ and $T = 25^0C$

## 6.3 Model extension

### *6.3.1 Extension of model for multiple-salts solution*

Since the osmotic pressure difference is the primary factor in PRO, this section shows the modeled osmotic pressure for high concentred draw and feed solution, which contains multiple ions (four cations: $Na^+$, $Mg^{2+}$, $Ca^{2+}$, $K^+$, and two anions: $Cl^-$, and $SO_4^{2-}$). The concentration of ions used for this study are shown in Table 6.1.

Table 6.1: Concentration of ions present in produced-water and seawater

| ions | Produced-water $gL^{-1}$ | Seawater $gL^{-1}$ |
|---|---|---|
| $Na^+$ | 40.15 | 10.8 |
| $Mg^{2+}$ | 2.415 | 1.29 |
| $Ca^{2+}$ | 14.065 | 0.416 |
| $K^+$ | 1.615 | 0.387 |
| $Cl^-$ | 90.22 | 19.51 |
| $SO_4^{2-}$ | 6.9 | 2.71 |

By utilizing the concentration of ions mentioned in Table 6.1, the osmotic pressure of both solutions were determined. At first, the calculation was done by the model developed in this study and then, compared with the results obtained from OLI-analyzer. The deviation between these two results were very low. The reason to compare the model results with OLI results is that OLI was also developed based on thermodynamic principles (UNIQUAC model). Table 6.3 shows the modeled osmotic pressure and the osmotic pressure calculated using OLI-analyzer.

Table 6.2: Concentration of ions present in produced-water and seawater

| | Osmotic pressure ($atm$) | | Deviation (%) |
|---|---|---|---|
| | Model | OLI | |
| Produced-water | 143.68 | 143.817 | 0.95 |
| Seawater | 27.16 | 25.97 | 4.58 |

### *6.3.2 Extension for two-stage membrane system*

In another investigation, the developed model was implemented on a two-stage PRO system. Three different configurations were studied, as mentioned in Section 5.3, and compared to a single-stage PRO performance. For this study, produced-water and seawater were used as the draw and feed solution respectively. Table 6.1 represents the concentration of the draw and feed solutions.

Table 6.3: Power density obtained for both single-stage and two-stage membrane systems with different configurations

| Configuration | Power density $Wm^{-2}$ |
|---|---|
| Single-Turbine | 10.37 |
| 2S1T | 6.71 |
| 2S2TP | 8.48 |
| 2S2T | 9.20 |

For single-stage calculation, the area of the membrane was $400m^2$, while for two-stage it was $200m^2$ each. The parameters and initial operating conditions of draw and feed solutions were same for this study.

# 7. CONCLUSION

Based on the results obtained in this study, some conclusions can be drawn:

- The mathematical model and modeling framework developed in this study can be used to estimate the overall performance of a PRO process. Both thermodynamic limiting performance and the detrimental effects of concentration polarization and reverse salt flux in the mass transfer can be estimated in a PRO process by simulation.

- Modeled osmotic pressure, water and salt fluxes, and power density for a single salt solutions are in very good agreement with the literature experimental and model results. Due to the scarcity of experimental data for the solutions of multiple ions, the modeled osmotic pressure is compared with the OLI results, which show the almost similar trend of osmotic pressure as a function of concentration.

- The osmotic pressure of the draw solution increases with increasing the concentration, thus improves the PRO performance. However, with increasing the concentration, the reverse salt flux across the membrane also increases. Contrarily, the increase in feed concentration reduces the osmotic pressure difference, thus reducing the power output from the process.

- The increase in flow rate of the solutions increases the power density of the process for a specific range of applied hydraulic pressure difference even though it slightly increases the salt flux across the membrane.

- Since the model predicts recoveries of energy from freshwater+seawater and seawater+brine that are in excellent agreement with the results of existing

models, it is applied to a high salinity system (produced-water+seawater). The developed model also can accurately calculate the thermodynamic properties and fluxes across the membrane needed to assess the performance of PRO plants.

- The developed model is extended for two-stage membrane with different flow configurations. Power density obtained for counter-current flow gives a good result compared to the co-current flow.

As last, we can say that the osmotic energy extraction and PRO are still at an early stage. They need extensive and in-depth investigations to increase the membrane power density and specific extractable energy, and to reduce the economic cost.

# 8. FUTURE WORK

In this thesis, a framework was established to predict different thermodynamic properties of electrolyte solutions and to determine water and salt fluxes, and power density simultaneously. However, many tests, analysis, and experiments were left for future due to lack of time. There are some possible directions that I would like to try for establishing an efficient PRO process:

1. This work mainly focuses on modeling of a PRO process; no experimental works are done in this study. Although some experimental results are available in the literature for low salinity solution, for higher salinity solution, no information have been found. Therefore, experiments should be conducted, especially for high salinity solutions that contains multiple salts, in order to validate the modeled results.

2. The existing membranes are suitable for low operating pressure conditions, even though the power density increases with increasing the operating pressure. In order to improve the membrane performance in PRO, innovative design and optimization of the membrane module should be developed.

3. Scaling and fouling are in PRO should be studied in greater depth because of their impact on performance.

4. This study mainly discusses the single-stage system and gives a very brief idea about the two-stage system. More investigations should be done for multiple-stage PRO systems.

# REFERENCES


[1] S. Shafiee and E. Topal, "When will fossil fuel reserves be diminished?," *Energy Policy*, vol. 37, no. 1, pp. 181–189, 2009.

[2] A. P. Straub, C. O. Osuji, T. Y. Cath, and M. Elimelech, "Selectivity and Mass Transfer Limitations in Pressure-Retarded Osmosis at High Concentrations and Increased Operating Pressures," *Environmental Science and Technology*, vol. 49, no. 20, pp. 12551–12559, 2015.

[3] A. Sharif, A. Merdaw, M. Aryafar, and P. Nicoll, "Theoretical and Experimental Investigations of the Potential of Osmotic Energy for Power Production," *Membranes*, vol. 4, no. 3, pp. 447–468, 2014.

[4] Y. C. Kim and M. Elimelech, "Potential of osmotic power generation by pressure retarded osmosis using seawater as feed solution: Analysis and experiments," *Journal of Membrane Science*, vol. 429, pp. 330–337, feb 2013.

[5] E. A. Emam, T. M. Moawad, and N. A. K. Aboul-gheit, "Evaluating the characteristics of offshore oilfield produced," *Petroleum & Coal*, vol. 56, no. 4, pp. 363–372, 2014.

[6] Y. C. Kim and M. Elimelech, "Potential of osmotic power generation by pressure retarded osmosis using seawater as feed solution: Analysis and experiments," *Journal of Membrane Science*, vol. 429, pp. 330–337, 2013.

[7] J. Veerman, M. Saakes, S. J. Metz, and G. J. Harmsen, "Reverse electrodialysis: Performance of a stack with 50 cells on the mixing of sea and river water," *Journal of Membrane Science*, vol. 327, no. 1-2, pp. 136–144, 2009.

[8] N. Y. Yip and M. Elimelech, "Thermodynamic and Energy Efficiency Analysis of Power Generation from Natural Salinity Gradients by Pressure Retarded Osmosis," 2012.

[9] T. Thorsen and T. Holt, "The potential for power production from salinity gradients by pressure retarded osmosis," vol. 335, pp. 103–110, 2009.

[10] A. Altaee and A. Sharif, "Pressure retarded osmosis: advancement in the process applications for power generation and desalination," in *Desalination*, vol. 356, pp. 31–46, Elsevier B.V., 2015.

[11] R. Rica, R. Ziano, D. Salerno, F. Mantegazza, R. van Roij, and D. Brogioli, "Capacitive Mixing for Harvesting the Free Energy of Solutions at Different Concentrations," *Entropy*, vol. 15, no. 4, pp. 1388–1407, 2013.

[12] M. C. Hatzell, R. D. Cusick, and B. E. Logan, "Capacitive mixing power production from salinity gradient energy enhanced through exoelectrogen-generated ionic currents," *Energy & Environmental Science*, vol. 7, p. 1159, 2014.

[13] R. Pattle, "Production of Electric Power by mixing Fresh and Salt Water in the Hydroelectric Pile," *Nature*, vol. 174, p. 660, 1954.

[14] S. Loeb, "Production of energy from concentrated brines by pressure-retarded osmosis," *Journal of Membrane Science*, vol. 1, pp. 49–63, jan 1976.

[15] J. W. Post, C. H. Goeting, J. Valk, S. Goinga, J. Veerman, H. V. M. Hamelers, and P. J. F. M. Hack, "Towards implementation of reverse electrodialysis for power generation from salinity gradients," *Desalination and Water Treatment*, vol. 16, no. 1-3, pp. 182–193, 2010.

[16] N. Y. Yip, A. Tiraferri, W. A. Phillip, J. D. Schiffman, L. A. Hoover, Y. C. Kim, and M. Elimelech, "Thin-film composite pressure retarded osmosis membranes for sustainable power generation from salinity gradients_," *Environmental Science and Technology*, vol. 45, no. 10, pp. 4360–4369, 2011.

[17] F. Helfer, C. Lemckert, and Y. G. Anissimov, "Osmotic power with Pressure Retarded Osmosis: Theory, performance and trends A review," *Journal of Membrane Science*, vol. 453, pp. 337–358, 2014.

[18] A. P. Straub, A. Deshmukh, and M. Elimelech, "Pressure-retarded osmosis for power generation from salinity gradients: is it viable?," *Energy Environ. Sci.*, 2015.

[19] A. Daniilidis, D. A. Vermaas, R. Herber, and K. Nijmeijer, "Experimentally obtainable energy from mixing river water , seawater or brines with reverse electrodialysis," *Renewable Energy*, vol. 64, pp. 123–131, 2014.

[20] G. Han, J. Zhou, C. Wan, T. Yang, and T. S. Chung, "Investigations of inorganic and organic fouling behaviors, antifouling and cleaning strategies for pressure retarded osmosis (PRO) membrane using seawater desalination brine and wastewater," in *Water Research*, vol. 103, pp. 264–275, Elsevier Ltd, 2016.

[21] C. F. Wan and T.-S. Chung, "Osmotic power generation by pressure retarded osmosis using seawater brine as the draw solution and wastewater retentate as the feed," *Journal of Membrane Science*, vol. 479, pp. 148–158, 2015.

[22] A. P. Straub, S. Lin, and M. Elimelech, "Module-Scale Analysis of Pressure Retarded Osmosis: Performance Limitations and Implications for Full-Scale Operation," *Environmental Science & Technology*, vol. 48, no. 20, pp. 12435–12444, 2014.

[23] S. Lin, A. Straub, and M. Elimelech, "Thermodynamic Limits of Extractable Energy by Pressure Retarded Osmosis," *Energy & Environmental Science*, vol. 7, no. 8, pp. 2706–2714, 2014.

[24] Q. She, X. Jin, and C. Y. Tang, "Osmotic power production from salinity gradient resource by pressure retarded osmosis: Effects of operating conditions and reverse solute diffusion," *Journal of Membrane Science*, vol. 401, pp. 262–273, 2012.

[25] E. M. Kramer and D. R. Myers, "Osmosis is not driven by water dilution," 2013.

[26] T. Y. Cath, A. E. Childress, and M. Elimelech, "Forward osmosis: Principles, applications, and recent developments," *Journal of Membrane Science*, vol. 281, no. 1, pp. 70–87, 2006.

[27] J. W. Post, J. Veerman, H. V. Hamelers, G. J. Euverink, S. J. Metz, K. Nymeijer, and C. J. Buisman, "Salinity-gradient power: Evaluation of pressure-retarded osmosis and reverse electrodialysis," *Journal of Membrane Science*, vol. 288, no. 1, pp. 218–230, 2007.

[28] E. Brauns, "Towards a worldwide sustainable and simultaneous large-scale production of renewable energy and potable water through salinity gradient power by combining reversed electrodialysis and solar power?," *Desalination*, vol. 219, no. 1-3, pp. 312–323, 2008.

[29] S. E. Skilhagen, J. E. Dugstad, and R. J. Aaberg, "Osmotic power - power production based on the osmotic pressure difference between waters with varying salt gradients," *Desalination*, vol. 220, no. 1-3, pp. 476–482, 2008.

[30] J. Veerman, M. Saakes, S. J. Metz, and G. J. Harmsen, "Reverse electrodialysis: A validated process model for design and optimization," *Chemical Engineering Journal*, vol. 166, no. 1, pp. 256–268, 2011.

[31] D. Brogioli, "Extracting renewable energy from a salinity difference using a capacitor," *Physical Review Letters*, vol. 103, no. 5, 2009.

[32] B. B. Sales, M. Saakes, J. W. Post, C. J. N. Buisman, P. M. Biesheuvel, and H. V. M. Hamelers, "Direct power production from a water salinity difference in a membrane-modified supercapacitor flow cell.," *Environmental Science and Technology*, vol. 44, no. 14, pp. 5661–5665, 2010.

[33] K. Lee, R. Baker, and H. Lonsdale, "Membranes for power generation by pressure-retarded osmosis," *Journal of Membrane Science*, vol. 8, pp. 141–171, jan 1981.

[34] G. D. Mehta and S. Loeb, "Internal polarization in the porous substructure of a semipermeable membrane under pressure-retarded osmosis," *Journal of Membrane Science*, vol. 4, no. C, pp. 261–265, 1978.

[35] S. Loeb and G. D. Mehta, "A two-coefficient water transport equation for pressure-retarded osmosis," *Journal of Membrane Science*, vol. 4, no. C, pp. 351–362, 1978.

[36] J. R. McCutcheon, R. L. McGinnis, and M. Elimelech, "A novel ammonia-carbon dioxide forward (direct) osmosis desalination process," *Desalination*, vol. 174, no. 1, pp. 1–11, 2005.

[37] G. T. Gray, J. R. McCutcheon, and M. Elimelech, "Internal concentration polarization in forward osmosis: role of membrane orientation," *Desalination*, vol. 197, no. 1-3, pp. 1–8, 2006.

[38] A. Achilli, T. Y. Cath, and A. E. Childress, "Power generation with pressure retarded osmosis : An experimental and theoretical investigation," *Journal of Membrane Science*, vol. 343, pp. 42–52, 2009.

[39] R. S. Norman, "Water salination: a source of energy," *Science*, vol. 186, no. June, pp. 350–352, 1974.

[40] S. L. Norman and R. S., "Osmotic Power Plants Author ( s ): Sidney Loeb and Richard S . Norman," *Science*, vol. 189, no. 4203, pp. 654–655, 1975.

[41] S. Loeb, T. Honda, and M. Reali, "Comparative mechanical efficiency of several plant configurations using a pressure-retarded osmosis energy converter," *Journal of Membrane Science*, vol. 51, no. 3, pp. 323–335, 1990.

[42] M. Reali, G. Dassie, and G. Jonsson, "Computation of salt concentration profiles in the porous substrate of anisotropic membranes under steady pressure-retarded-osmosis conditions," *Journal of Membrane Science*, vol. 48, no. 2-3, pp. 181–201, 1990.

[43] S. Loeb and G. Bay, "One hundred and thirty benign and renewable megawatts from Great Salt Lake ? The possibilities of hydroelectric power by pressure-retarded osmosis," vol. 141, pp. 85–91, 2001.

[44] S. Loeb, "Large-scale power production by pressure-retarded osmosis, using river water and sea water passing through spiral modules," *Desalination*, vol. 143, pp. 115–122, may 2002.

[45] Q. She, D. Hou, J. Liu, K. H. Tan, and C. Y. Tang, "Effect of feed spacer induced membrane deformation on the performance of pressure retarded osmosis (PRO): Implications for PRO process operation," *Journal of Membrane Science*, vol. 445, pp. 170–182, 2013.

[46] J. Ali and A. Semwal, "Renewable energy in India: Historical developments and prospects," *International Journal of Applied Engineering Research*, vol. 9, no. 10 SPEC. ISSUE, pp. 1169–1183, 2014.

[47] S. C. Chen, G. L. Amy, and T. S. Chung, "Membrane fouling and anti-fouling strategies using RO retentate from a municipal water recycling plant as the feed for osmotic power generation," *Water Research*, vol. 88, pp. 144–155, 2016.

[48] A. Altaee, G. Zaragoza, and A. Sharif, "Pressure retarded osmosis for power generation and seawater desalination: Performance analysis," *Desalination*, vol. 344, pp. 108–115, 2014.

[49] A. Altaee and N. Hilal, "Dual-stage forward osmosis/pressure retarded osmosis process for hypersaline solutions and fracking wastewater treatment," *Desalination*, vol. 350, pp. 79–85, 2014.

[50] A. Zuber, R. F. Checoni, and M. Castier, "Thermodynamic properties of aqueous solutions of single and multiple salts using the Q-electrolattice equation of state," *Fluid Phase Equilibria*, vol. 362, no. 0, pp. 268–280, 2014.

[51] P. Debye and E. Hückel, "On the Theory of Electrolytes. I. Freezing Point Depression and Related Phenomena," *Physikalische Zeitschrift*, vol. 24, pp. 185–206, 1923.

[52] M. Born, "volumen und hydratationswärme der ionen," *Zeitschrift für Physik*, vol. 1, no. 1, pp. 45–49, 1920.

[53] E. Martina and F. del R??o, "An interpretation of the mean spherical approximation," *Physics Letters A*, vol. 53, no. 5, pp. 355–356, 1975.

[54] J. F. Lu, Y. X. Yu, and Y. G. Li, "Modification and application of the mean spherical approximation method," *Fluid Phase Equilibria*, vol. 85, no. C, pp. 81–100, 1993.

[55] D. M. Zuckerman, M. E. Fisher, and B. P. Lee, "Critique of Primitive Model Electrolyte Theories," *Physical Review E*, vol. 56, no. 6, p. 13, 1997.

[56] S. Mattedi, F. Tavares, and M. Castier, "Calculation of mixture critical diagrams using an equation of state based on the lattice fluid theory," *Brazilian Journal of Chemical Engineering*, vol. 17, pp. 771–784, dec 2000.

[57] a. Zuber, R. Checoni, R. Mathew, J. Santos, F. Tavares, and M. Castier, "Thermodynamic Properties of 1:1 Salt Aqueous Solutions with the Electrolattice Equation of State," *Oil & Gas Science and Technology Revue d'IFP Energies nouvelles*, vol. 68, no. 2, pp. 255–270, 2013.

[58] A. Zuber, R. Figueiredo, and M. Castier, "Fluid Phase Equilibria Thermodynamic properties of aqueous solutions of single and multiple salts using the Q-electrolattice equation of state," *Fluid Phase Equilibria*, vol. 362, pp. 268–280, 2014.

[59] J. a. Myers, S. I. Sandler, and R. H. Wood, "An Equation of State for Electrolyte Solutions Covering Wide Ranges of Temperature, Pressure, and Composition,"

*Industrial & Engineering Chemistry Research*, vol. 41, no. 13, pp. 3282–3297, 2002.

[60] Y. Marcus, "Ionic Radii in Aqueous Solutions," vol. 12, no. 4, pp. 271–275, 1988.

[61] M. Castier and M. M. Amer, "XSEOS: An evolving tool for teaching chemical engineering thermodynamics," *Education for Chemical Engineers*, vol. 6, no. 2, pp. e62–e70, 2011.

[62] M. Hamdan, A. O. Sharif, G. Derwish, S. Al-Aibi, and A. Altaee, "Draw solutions for Forward Osmosis process: Osmotic pressure of binary and ternary aqueous solutions of magnesium chloride, sodium chloride, sucrose and maltose," *Journal of Food Engineering*, vol. 155, pp. 10–15, 2015.

# APPENDIX A

## FOSSIL FUELS PRODUCTION VERSUS CONSUMPTION

This appendix includes the trends of world fossil fuels proven reserve and their consumption over a specific time period [1]. The information are collected from EIA (U.S. Energy Information Administration) and BP (British Petroleum).

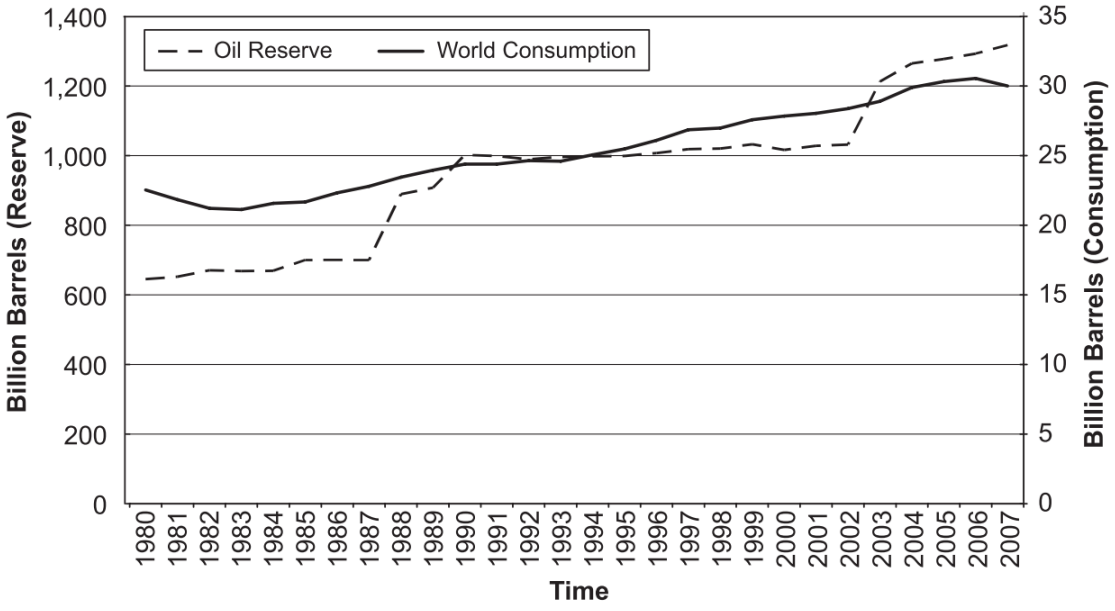


Figure A.1: Trends of world crude oil proven reserves and oil consumption from 1980 to 2007.

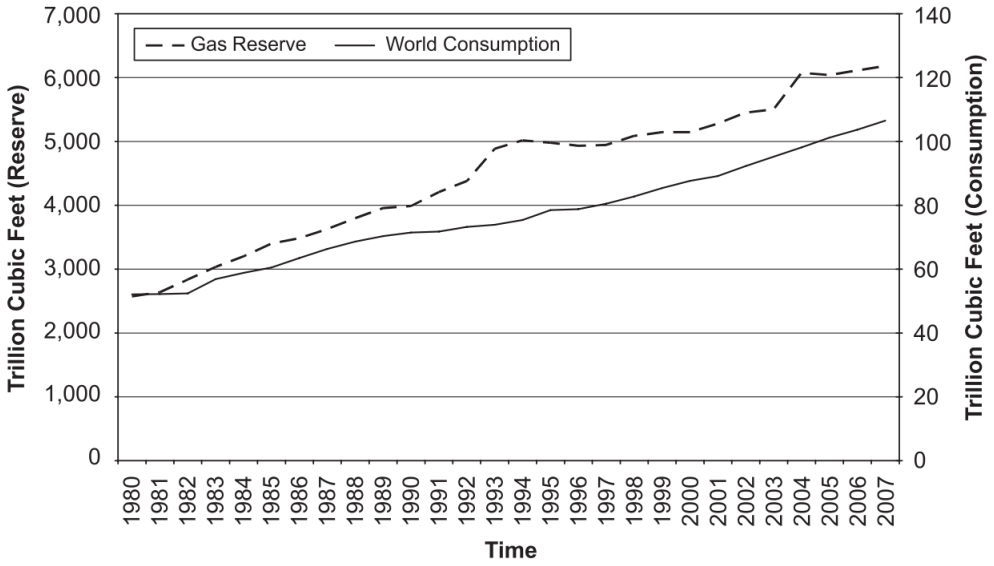


Figure A.2: Trends of world natural gas proven reserves and gas consumption from 1980 to 2007.

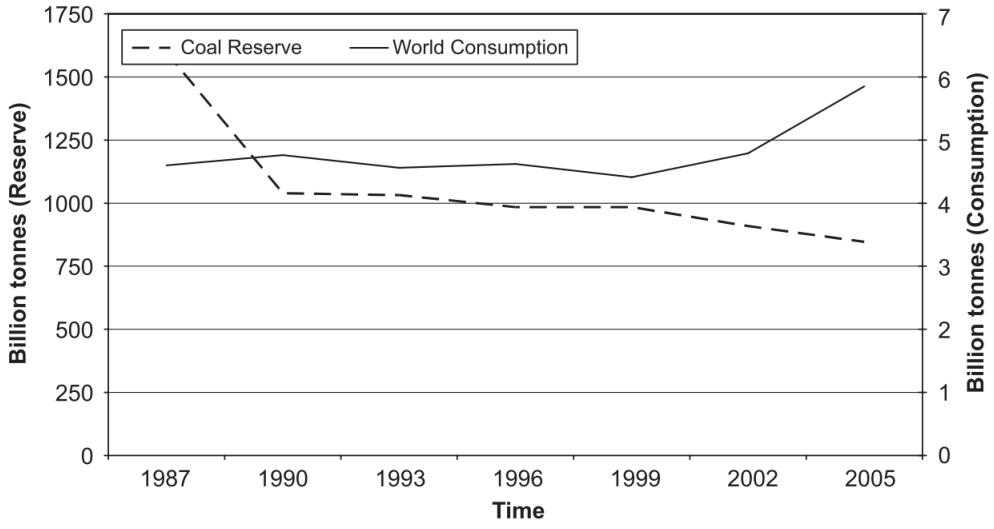


Figure A.3: Trends of world coal proven reserves and coal consumption from 1987 to 2005. Data

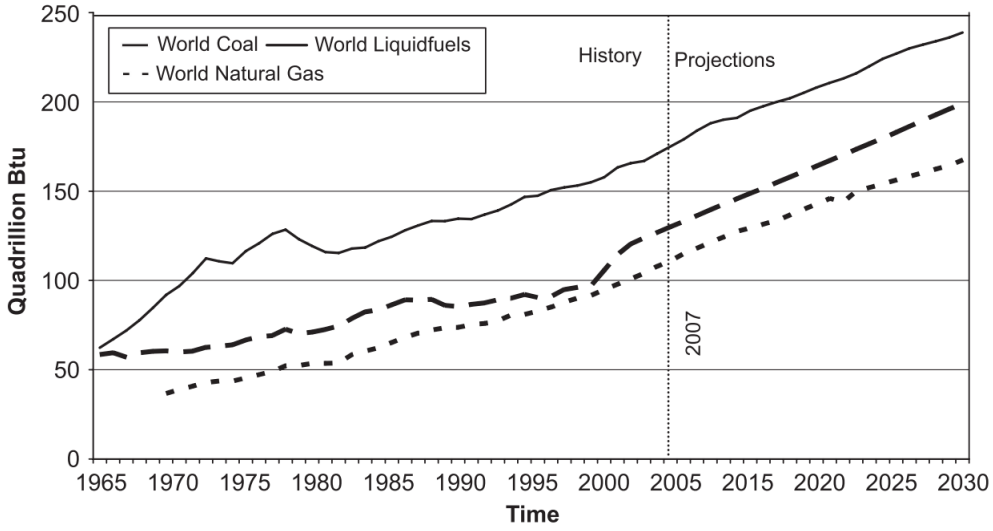


Figure A.4: Consumption of fossil fuel worldwide from 1965 to 2030.